JOVE Final Report

Name: Stephen Schiller
Institution: South Dakota State Univ.
Date:12\20\97

I. Research

Brief description of research results to date on your project: (100 words or less)

The focus of our JOVE research has been to develop a field instrument that provides high quality data for atmospheric corrections and in-flight calibration of airborne and satellite remote sensing imaging systems. The instrument package is known as the Portable Ground-based Atmospheric Monitoring System or PGAMS. PGAMS collects a comprehensive set of spectroscopic/radiometric observations that describe the optical properties of the atmosphere and reflectance of a target area on the earth's surface at the time of the aircraft or satellite overpass. To date, the PGAMS instrument system and control software has been completed and used for data collection in several NASA field experiments across the continental US and Puerto Rico.

Where do you see your JOVE research going after the initial JOVE Funding Expires?

Our JOVE initiated research will continue to be very active in supporting validation and calibration activities in remote sensing involving NASA, DOE, DOD, NSF, and possibly commercial supported programs. Future effort will focus on projects related to NASA's Mission to Planet Earth. This will include field work using PGAMS and data analysis that evaluates sensor calibration and atmospheric effects in images recorded by ASTER, MODIS, and MISR instruments aboard the AM-1 platform.

Communication with NASA Colleague
(Please indicate the extent of your contact with your NASA colleague. Is the communication producing qualitative results? Do you still consider the match to be viable, and do you anticipate continuing your research collaboration after formal JOVE funding expires)

The communication and overall interaction with Jeff Luvall on this project has been excellent. We are in touch regularly and continue to collaborate in research. Both of us have worked together in several field experiments and have co-authored several papers. We anticipate that this relationship will continue long into the future.

Refereed Journal Articles Published: (title, authors, journal, date, and attach a copy of the full publication)

Milone, E.F., Wilson, W.J.F., Fry, D.J.I., Schiller, S.J. 1994, "Studies of Large Amplitude Delta Scuti Variables II: DY Herculis", Publications of the Astronomical Society of the Pacific, 106, 1120.

"Studies of Large Amplitude Delta Scuti Variables II: DY Herculis", Publications of the Astronomical Society of the Pacific, 106, 1120.

Milone, E.F., Stagg, C.R., Sugers, B.J.A., McVean, J.R., Schiller, S.J., and Kallrath, J. 1995, "Observations and Analysis of the Contact Binary H235 in the Open Cluster NGC 752", Astronomical Journal, 109, 359.

Schiller, S.J., Bridges, D., and Clifton, T., 1996, "New Photometric Light Curve Measurements of SS Lacertae from the Harvard College Observatory Plate Archives", in Origins, Evolution, and Destinies of Binary Stars in Clusters, E.F. Milone and J.-C. Mermilliod, eds.,(Astron. Society of the Pacific: San Francisco), pp. 141-143,1996.

Schiller, S.J., and E,F. Milone 1996, "Binaries in Clusters: Exploring Binary and Cluster Evolution", in Origins, Evolution, and Desinies of Binary Stars in Clusters, E.F. Milone and J.-C. Mermilliod, eds.,(Astron. Society of the Pacific: San Francisco), pp. 120-130, 1996.

Schiller, S.J. 1996, "Cosmic Billiards", Astronomy Magazine, July Issue, 104, pp.46-49.

Schiller, S.J. and Luvall, J. 1996, "Evaluation of the Aerosol Scattering Phase Function from PGAMS Observations of Sky Path Radiance", in the proceedings of IGARSS96: Remote Sensing for a Sustainable Future, Lincoln, Nebraska, pp.1286-89.

Schiller,S.J., Luvall, J., and Justus, J. 1996, "Calibration of MODTRAN3 with PGAMS Observational Data for Atmospheric Corrections Applications", Proceedings of SPIE, Vol. 2758, pp. 366-374

Refereed Journal Articles Submitted: (title, authors, journal, date submitted)

Other Publications Publisbed: (i.e. abstracts, technical memorandums)
Milone, E.F., Stagg, C.R. and Schiller, S.J. 1992, "Constraints on the Cessation Of Eclipses in SS Lacertae and Their Implications for System Evolution", in IAU Symposium No. 151 Evolutionary Processes in Interacting Binary Stars, August 5-8, 1991, Cordoba, Argentina, pages 479-82.

Milone, E.F., McVean, J.R. Lu, W., Schiller, S.J. and Miller, G. 1994, "The Binaries-in-Clusters Program in the Age of Imaging", IAU Symposium #161, Astronomy from Wide-Field Imaging, August 23-27, 1993, Berlin, Germany.

Schiller, S.J., and Luvall, J. 1994, " A Portable Ground-based Atmospheric Monitoring System (PGAMS) for the calibration and validation of atmospheric correction algorithms applied to satellite images", Proc. SPIE, 2231, pages 191-98.

Oral and Poster Papers Presented: (title, date, conference name, etc., include co-authored presentations, and attach a copy of the abstract)

Proposals Awarded: (attach the signature page, title page, and table of contents)

1. Agency providing funding: USGS $ amount:$75,590

Title of project/PI: Relative Radiometric Calibration of the Landsat Archive / Dennis Helder and Stephen Schiller

Period of Performance: 9/1/94 to 5/31/95

Primary Use of Funds: Release time salaries for PI's and student support

2. Agency providing funding: French Centre National d'Etudes Spatiales (CENS) $ amount:$332,600

Title of project/PI: Monitoring Seasonal Dynamics of North American Grasslands Using VEGETATION /David J. Meyer et al.

Period of Performance: 2/95 to 11/98

Primary Use of Funds: Purchase of satellite images and field equipment

3. Agency Providing Funding: NSF/South Dakota EPSCoR $ amount:$944,109

Title of project/PI: Comprehensive Investigation of the Instrumental and Atmospheric Point-Spread Function Affecting Ground-based, Airborne, and Satellite Environmental Observations / Dennis Helder, Stephen Schiller, Sung Shin (SDSU)

Period of Performance: 6/95 to 6/98

Primary Use of Funds: Salaries, equipment, and student support.
The amount given above is the three year budget for our investigation alone that has been approved by NSF.

Proposals Submitted:

1. Agency Submitted to:USDA $ amount $50,000

Title/PI: Carbon Isotope Measurements from Remotely Sensed Reflectance Spectra/ Kevin Kephart and Stephen Schiller

Period of Performance:10/95 to 10/97

Primary Use of Funds: Salary and student support

Status: Was not funded

2. Agency Submitted to: US Department of Energy $ amount: $600,00

Title/PI: An Advanced Portable Ground-Based Atmospheric Monitoring System(PGAMS) for hyperspectral Angular Measurements of Shortwave Radiative Fluxes/ Stephen Schiller and Jeff Luvall

Period of Performance:10/97 to 10/00

Primary Use of Funds: Equipment and Salary

Status: Was not funded.

3. Agency Submitted to: NASA's Office of Mission to Planet Earth

$ amount: $387,000

Title/PI: A Radiometer Network for the Areal Validation of EOS Products / Stephen Schiller

Period of Performance: 10/97 to 10/00
Primary Use of Funds: Salary, Student Support, and Equipment

Status: Was not funded.

4. Agency Submitted to: DOD EPSCoR Program $ amount: $437,220

Title/PI: Validation of Atmospheric Remote Sensing Image Restoration and Moisture Retrieval

Period of Performance: 4/98 to 4/01
Primary Use of Funds: Salary, Student Support, and Equipment

Status: In review process.

Are you utilizing the Internet or other network? If other, which?

Internet - for e-mail, data transfer, and remote log in to MSFC computers.

Please identify the data sets, if any, used in your research.

II. Education:

Assessment of Student Impact: Indicate the impact, if any, that the JOVE Program has had on student enrollment and/or recruitment. Please provide before and after numbers for science majors by discipline, course enrollment, etc.

The impact has been to greatly increase opportunities for research to be a part of the undergraduate educational experience at SDSU for our majors.

Student Research Assistants (Please complete the attached form for each student listed below.)

Undergraduate Assistants:	Research Area:	Major:
Corey Plender	Instrument Control in Remote Sensing	Engineering Physics / Electrical Eng.
Tammy Clifton	Stellar Astrophysics	Physics

Presentations:

Title: The Disappearance of Eclipse Minima of the Binary Star SS Lacertae

American Association of Physics Teachers / Society of Physics Students, Regional Meeting, Sioux Falls, SD, November 12, 1994.

National Conference of Undergraduate Research, Schnectady, NY, April 20, 1995.

Publications:

Title: The Disappearance of Eclipse Minima of the Binary Star SS Lacertae

National Conference of Undergraduate Research Proceedings, 1995 (In Press).

Steve Fox	Remote Sensing	Engineering Physics / Mathematic
Cameron Havlik	Stellar Spectroscopy	Engineering Physics /Electrical Eng.
Graduate Assistants:	**Research Area:**	**Major:**
Dallas Bridges	Image Processing	Engineering Physics / Electrical Eng.
Weixing Shen	Scattering of light In the Earth's Atmosphere	Engineering Physics
Zhaohui Wang	Reflectance Spectra of The Earth's Surface	Engineering Physics / Computer Science

III. Curriculum Development

New Curricula: (Please list any new majors, minors, or areas of concentration which have been implemented as a result of your institution's participation in JOVE. Indicate current student enrollments, and attach a copy of the new curricula description from your institution's course catalogue.)

New Courses: (course title, department, student enrollments, attach copy of course syllabus and catalog description)

Course title: Physics 598/698 Photonics
Department: Physics
Student enrollment: 8 - 10

Course was added in part because of increased student interest and research involvement in optical measurement and instrumentation resulting from the JOVE program at SDSU.

Amended Courses or Augmented Courses: (list new topics included, student enrollments and attach a copy of the course syllabus)

☐

☐

☐

☐

Reading or independent study courses: (course title, department, student enrollments and attach a copy of the course syllabus)

☐

☐

☐

IV. Outreach

Please indicate your outreach efforts in each of the categories below. List the type of outreach effort (lecture, workshop, etc.), location, and estimated number of attendees.

Students: (high school, middle, elementary, other)

Outreach Effort	Location	Estimated number of Attendees
1. South Dakota Space Day Exhibit	Pierre (April 1995)	1500

The members of the South Dakota Space Grant Consortium (SDSU, SD School of Mines and Technology, and EROS Data Center) sponsored Space Day to promote space related activities in South Dakota. Teachers and students in schools across South Dakota were invited. Our participation involved an exhibit of JOVE research activities under the title of Astrophysics and Space Science Laboratory, SDSU (see attached brochure). The exhibit included a

poster presentation of JOVE research and hands on computer activities for displaying properties of binary stars and the dynamics of earth orbiting satellites. JOVE students, Tammy Clifton and Steve Fox participated in manning the exhibit

2. Science Week Lectures and Demontrations	Brookings Central Elementry School	50

Was a presenter during "Science Week" at the Brookings Central Elementary School in March 1994. Worked with 3rd grade students for 4 days in two 45 min sessions/day. Under the topic "Physics and the Conservation of Energy" numerous demonstrations were conducted, many of them hands-on. Some of the discussions centered around space science related topics such as the propulsion of rockets and energy from the sun.

3. South Dakota Space Day Exhibit	Augustana College Sioux Falls, SD April 24, 1997	2000

The members of the South Dakota Space Grant Consortium (SDSU, SD School of Mines and Technology, and EROS Data Center) sponsored Space Day to promote space related activities in South Dakota. Teachers and students in schools across South Dakota were Invited and several thousand students attended from K-12. Our participation involved an exhibit of JOVE research activities dealing with the measurements of solar radiation in the Earth's atmosphere. Field equipment used to make measurements were displayed and demonstrated.

Teachers: (high school, middle, elementary, other)

Outreach Effort	Location	Estimated number of Attendees
1. South Dakota Space Day 95 (see above)	Pierre	1500
2. South Dakota Space Day 97	Sioux Falls	2000
3.		

Public: (civic, professional organizations, etc.)

Outreach Effort	Location	Estimated number of Attendees
1.Professional Workshop	EROS Data Center	30

Presentation of a workshop at EROS Data Center, August 15-17,1994, by Dennis Helder, Wayne Bonzyk, and myself dealing with calibration of remote sensing systems. Approximately 30 participants included leading scientists in this field from across the US and Canada. I lead out in the discussion topic "Calibration and Cross-Calibration of Ground Equipment" and demonstrated the PGAMS equipment.

2.

3.

V. Summer Programs: (describe program, location, date(s), # of attendees, length of program, etc.)

For students:

For teachers:

VI. "Roadblocks" to Progress/Suggestions

VII. How could the program be changed to make it more effective

Make it possible for mentors to attend the annual Jove conferences.

VII. Overall, what has been your institution's greatest benefit from participating in JOVE.

The greatest benefit is the administrative and funding infrastructure that the JOVE program sets up between NASA and the JOVE participant's home institution to conduct a meaningful research program that includes significant student participation.

IX. Please list all subject inventions as a result of this award or provide a statement that there were none.

VII. Other Activities

Collected PGAMS data in Sept. 1994 supporting the Research Project "Analysis of Urban Heat Island Development over Huntsville, Alabama Using Remote Sensing Data". The PI's are Dale Quattrochi and Jeff Luvall of MSFC with funding from the MSFC Director's Discretionary Fund. The PGAMS data is being used for atmospheric corrections and sensor calibration. The project had a unique component that involved hundreds of K-12 students through out the Huntsville area in collecting and analyzing data

for the study. This work continued with a study of the city of Atlanta in 1996 and 1997.

A major effort was made to expand our application of the PGAMS system by developing a strong collaboration effort with Remote Sensing Group at the University of Arizona under the direction of Phil Slater. The Remote Sensing Group has the major responsibility of characterizing and monitoring radiometric calibration of several sensors to be flown on EOS platforms and currently performs ground-based in-flight calibration of the SPOT and Landsat 5 remote sensing systems. The PGAMS system was transported to White Sands, New Mexico, where we conducted a joint field campaign for Spot and Landsat radiometric calibration in April, 1995. The capabilities of the PGAMS atmospheric and surface measurements will be compared to the measurements obtained by the Remote Sensing Group for quality of measurements and future potential of PGAMS as a principle field instrument in support of the EOS mission. This activity continued with field campaigns at Lunar Lake, Nevada in June of 1996 and 1997 to develop techniques for absolute vicarious calibration of the EOS sensor MODIS, MISER and ASTER.

Calibration of MODTRAN3 with PGAMS Observational Data for Atmospheric Correction Applications

Stephen Schiller

Physics Department, South Dakota State University
Brookings, SD 57007

Jeff Luvall and Jere Justus

Global Hydrology & Climate Center
NASA, Marshall Space Flight Center
977 Explorer Blvd., Huntsville, AL 35806

ABSTRACT

The Portable Ground-based Atmospheric Monitoring System (PGAMS) is a spectroradiometer system that provides a set of *in situ* solar and hemispherical sky irradiance, path radiance, and surface reflectance measurements. The observations provide input parameters for the calibration of atmospheric algorithms applied to multispectral and hyperspectral images in the visible and near infrared spectrum. Presented in this paper are the results of comparing hyperspectral surface radiances calculated using MODTRAN3 with PGAMS field measurements for a blue tarp and grass surface targets. Good agreement was obtained by constraining MODTRAN3 to only a rural atmospheric model with a calibrated visibility and surface reflectance from PGAMS observations. This was accomplished even though the sky conditions were unsteady as indicated by a varying aerosol extinction. Average absolute differences of 11.3 and 7.4 percent over the wavelength range from 400 to 1000 nm were obtained for the grass and blue tarp surfaces respectively. However, transformation to at-sensor radiances require additional constraints on the single-scattering albedo and scattering phase function so that they exhibit the specific real-time aerosol properties rather than a seasonal average model.

1. INTRODUCTION

Real-time monitoring of the optical properties of the atmosphere from the Earth's surface will be an important part of the coming Mission to Planet Earth. Atmospheric corrections over land and in-flight absolute calibration of EOS sensors will be the main beneficiaries of such a monitoring program.

0-8194-2139-1/96/$6.00

The objective is to the provide accurate quantitative data for remote sensing investigations using satellite and airborne remote sensing images. This is best accomplished when direct observations are obtained that characterize the optical properties of the atmosphere at the time and place a remote sensing image is acquired. In turn, these are used to constrain a radiative transfer code. The resulting calculations make it possible to convert radiances measured at the sensor to surface reflectance and upwelling radiance or to predict at-sensor radiances for vicarious calibration using the measured surface reflectance of a calibration target. Our objective is to develop this capability with hyperspectral resolution.

The purpose of this paper is to present initial results working with ground truth data collected with the Portable Ground-based Atmospheric Monitoring System (PGAMS)[1]. PGAMS observations of atmospheric transmission and surface reflectance are used to calibrate MODTRAN3[2,3] and predict upwelling radiances from a blue nylon tarp and grass targets. The resulting synthetic radiance spectra are compared to direct at-surface measurements obtained with PGAMS. This was done is to evaluate the ability of MODTRAN3 to model observed atmospheric optical conditions and to predict at-sensor radiances.

Of particular interest is the ability of PGAMS to obtain sufficient observations for atmospheric correction in a real world atmosphere. Generally, atmospheric corrections techniques are validated at high altitude sites under very clear cloudless sky conditions. However, most quantitative investigations by the users of remote sensing data will not be situated in such an ideal environment. The need is to develop a capability for atmospheric correction under non-ideal sky conditions. The data set used in this study was obtained in a clear but unstable atmosphere at Huntsville, Alabama.

2. DESCRIPTION OF EXPERIMENT

2.1. Instrumentation

All the measurements of atmospheric optical properties for this investigation were obtained with the PGAMS field instrument. Calibrated irradiance, radiance, and reflectance observations are recorded using a single diode-array field spectrometer[4] (Personal Spectrometer 2) providing radiometric measurements in 512 channels over the wavelength range of 350 to 1050 nm in 1.4 nm steps. An alt-alt tracking system controls the altitude and azimuth pointing of the spectrometer's 1 degree field-of-view (FOV) foreoptics with an angular resolution of 20 arcseconds. Additional foreoptics can provide 5°, 10°, 18°, and 180° FOV input through a fiber optic feed. An additional 10-channel sunphotometer is typically run to record continuous observations of the direct normal solar flux but it did not provide any data for this report due to computer problems. Overall, the PGAMS instrument was used to obtain hyperspectral measurements of:

1) Direct solar irradiance,
2) Diffuse sky irradiance,
3) Diffuse to global ratio,
4) Sky path radiance as a function of altitude and azimuth including almucantar scans and hemispherical sky radiance maps, and
5) Surface reflectance observations when detached from the alt-alt mounting.

All of these observations were recorded with the same spectroradiometer detector for the purpose of reducing the difficulties inherent when comparing data measured by independent detectors.

2.2. Field Campaign

Spectroradiometric observations were collected using PGAMS in support of a field campaign dealing with the analysis of urban heat island development around Huntsville, Alabama on September 7, 1994. The objective was to provide atmospheric correction and in-flight calibration for image data obtained with the Airborne Thermal/Visible Land Application Sensor (ATLAS). Application of the PGAMS data to the calibration of ATLAS imagery will be presented in a future publication.

This presentation concentrates on the radiative transfer properties of the atmosphere and two surfaces used as calibration targets. The surfaces were a 60 by 80 foot blue tarp and a 100 by 160 foot surface of grass covered soil. PGAMS observations of reflectance and upwelling radiance were recorded for both. The following radiative transfer analysis was conducted for the solar geometry and atmospheric conditions at the mid-time the surface measurements for each target were recorded.

3. USING PGAMS OBSERVATIONS TO CALIBRATE RADIATIVE TRANSFER CALCULATIONS

3.1. Atmospheric Conditions

The atmospheric conditions on Sept. 7, 1994 were far from ideal. It reflects the difficulties that are typical with real world field campaigns conducted in rural and urban environments. Though the skies were cloud free throughout the day, erratic temporal variations in the aerosol transmittance significantly affected the magnitude of the direct solar irradiance reaching the earth's surface. Thus, the following radiative transfer modeling will be done so as to be specific to the atmospheric conditions at the mid-time the reflectance spectra were recorded for the grass and blue tarp targets. Figure 1 shows the temporal variability of the direct solar irradiance measured with PGAMS at a wavelength of 500 nm. Significant variations in aerosol extinction are present and will be the dominant source of error in the atmosphere model calculations.

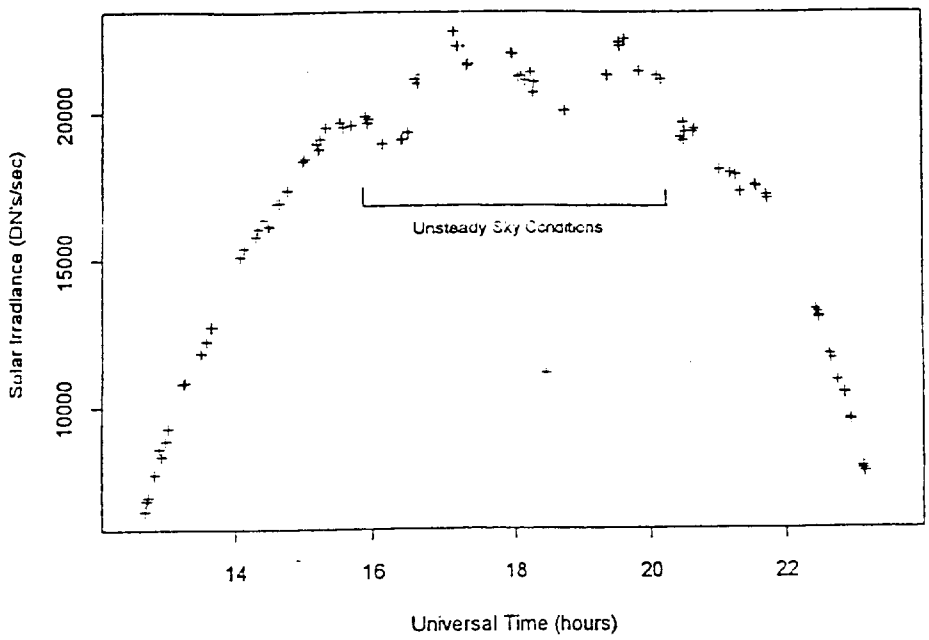

Figure 1. Temporal variations in direct normal solar irradiance on Sept. 7, 1994 recorded at 500 nm. Units are instrumental raw digital numbers.

3.2. Measurements of target spectral reflectance.

The upwelling radiance and spectral reflectance of the grass and blue tarp targets were measured with the PS2 using an 18° FOV foreoptic about 2 meters above the surface. The view geometry was nadir and normal to the target surface. Several hundred spectra were averaged together that were uniformly sampled over the surface area. It took 6 minutes and 4 minutes respectively to sample each surface at median times of 19.02 and 19.11 hours UT. The solar zenith angle at mid-sample time was 33.82° and 34.97° respectively. The resulting average reflectance spectra are shown in Figure 2 determined with reference to a calibrated spectralon panel.

3.3. Calibrating MODTRAN3 to fit the observed transmittance spectrum

The process of calibrating MODTRAN3 to model the observed atmospheric conditions will be based principally on determining the correct surface range or visibility (VIS) of the aerosol boundary layer. Using the exoatmosphere solar irradiance from standard Langley plot calibration of the PGAMS spectrometer, the aerosol extinction coefficients and the MODTRAN visibility parameter can be estimated from individual solar irradiance spectra. The atmospheric transmittance spectrum corresponding to the median time of the blue tarp and grass reflectance observations was determined from linear interpolation of solar irradiance spectra recorded at 18.748 and 19.364 hours UT. With some fine tuning of the visibility parameter, a match between the observed PGAMS and synthetic MODTRAN spectrum was evaluated for the time of the grass and blue tarp reflectance observations. The comparison is made only for channels where water vapor absorption is negligible. In

this way, a visibility of 37.1 km and 41.0 km were determined for 19.02 and 19.11 hours UT respectively. The resulting fit of the PGAMS and MODTRAN3 spectra for the mid-time of the grass reflectance observations is shown in Figure 3. The 1976 standard atmosphere with a spring-summer rural aerosol was selected for the MODTRAN3 calculation.

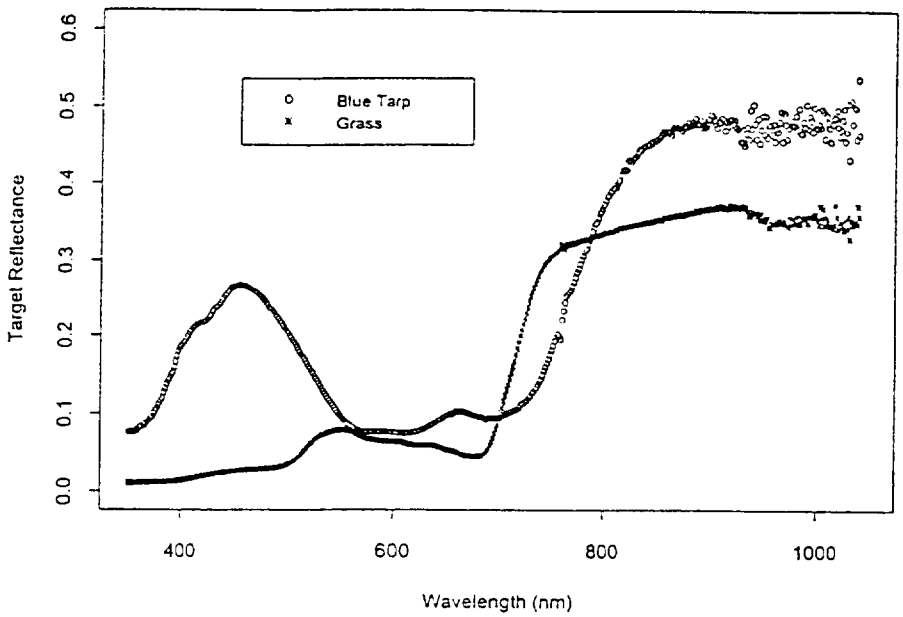

Figure 2. Calibrated average reflectance spectra of the blue tarp and grass targets measured with PGAMS.

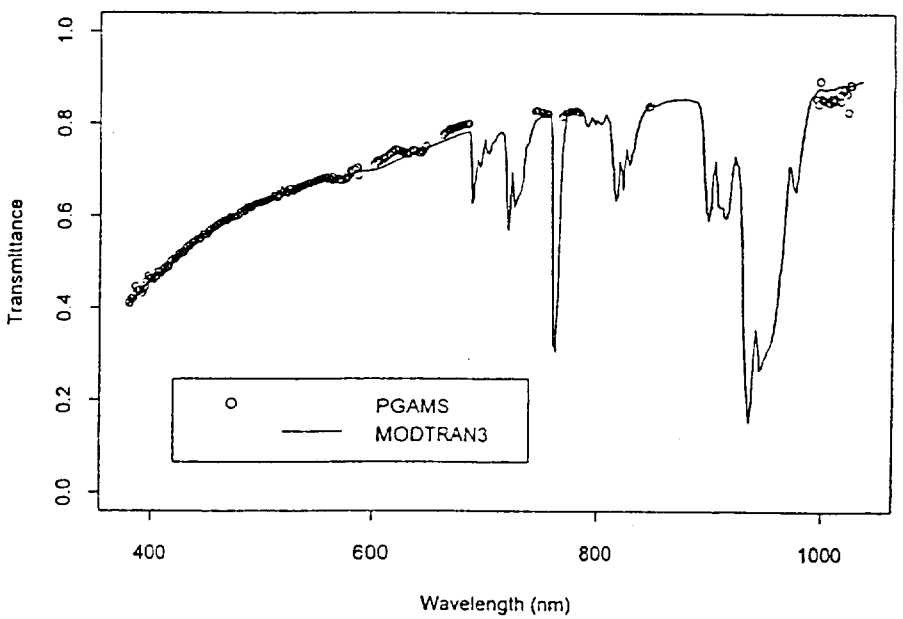

Figure 3. MODTRAN3 transmittance spectrum for VIS = 37.1 km compared to PGAMS measured transmittance at 19.02 hours UT.

4. SURFACE RADIANCE: COMPARISON BETWEEN OBSERVATION AND MODEL

MODTRAN3 was set up to duplicate the same view geometry as seen by the PS2 when it recorded the radiance and reflectance from above the grass and blue tarp targets. The model was calibrated with the visibility, solar zenith angle, and spectral surface reflectance for each target and time of observation. The two-stream multiple scattering mode was also used. The resulting synthetic spectra of the upwelling radiance is shown for the two surfaces in Figures 4 and 5. Direct comparison is made with the PGAMS observations. The PGAMS measurements of the upwelling radiance were transformed from instrumental to absolute units using coefficients derived from calibration lamp measurements. The absolute radiance calibration was conducted with a LI-COR Optical Radiation Calibrator providing an accuracy of better than +/- 5% using a NIST secondary standard lamp.

The agreement between the observed and synthetic surface radiance spectra reflects an average absolute difference of 11.3 and 7.4 percent between 400 and 1000 nm for the grass and blue tarp targets respectively. This comparison is very good considering the unstable sky conditions. The largest systematic difference is in the near infrared where the aerosol properties begin to dominate the extinction and scattering processes. It results from the likelihood that the aerosol model used in MODTRAN3 does not adequately represent the actual aerosols present in the atmosphere. Further analysis will be conducted using the constant altitude scans of sky path radiance and diffuse to global ratio to evaluate a single-scattering albedo and scattering phase function that is a better representation of the actual aerosol properties.

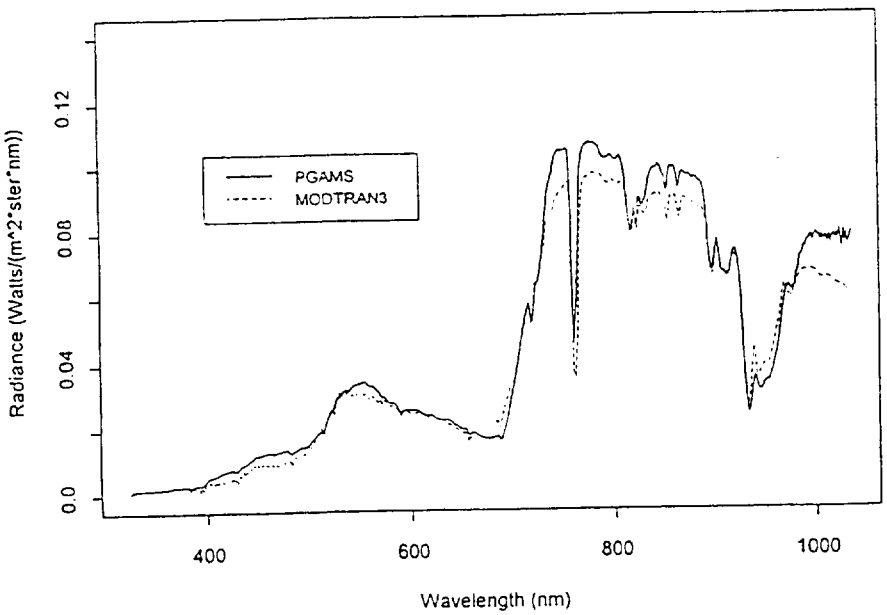

Figure 4. PGAMS measured upwelling radiance from the grass target area compared to the predicted MODTRAN3 radiance.

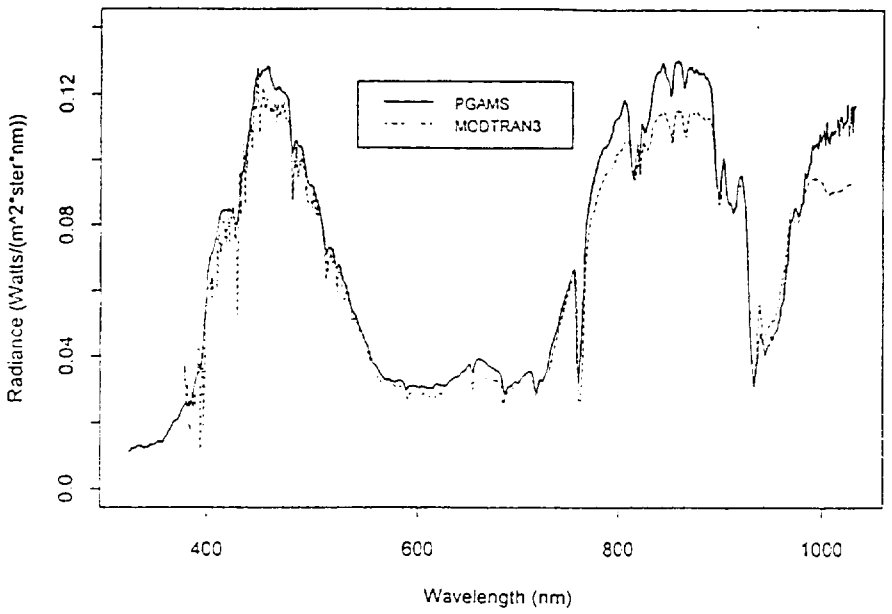

Figure 5. PGAMS measured upwelling radiance from the blue tarp target compared to the predicted MODTRAN3 radiance

Based on the results presented in Figures 4 and 5, one recognizes that MODTRAN3 is modeling the radiative transfer processes that propagate the solar radiation from the top of the atmosphere to the ground and than scattered off the target surface with good success. As a result, one would expect the same model to also propagate the surface radiance to the overflying sensor with similar accuracy. However, the transmitted surface radiance will not be the only component contributing to the observed at-sensor radiance. Single and multiple scattering by aerosols will introduce a large path radiance component to the at-sensor signal. Thus, the problem of using only a seasonal average aerosol model provided in MODTRAN3 may introduce significant error in the predicted path radiance component of the at-sensor radiance. The next section of this paper looks into this concern.

5. EVALUATING THE PATH RADIANCE CONTRIBUTION TO AT-SENSOR RADIANCE CALCULATIONS

The calibrated MODTRAN3 atmosphere can be used to calculate the surface radiance reaching the altitude of a remote sensing system (L_{surf}). However, the total radiance detected by the sensor (L_{sen}) will also include the path radiance produced by solar radiation scattered into the sensor's field-of-view by the atmosphere (L_{atm}). These three quantities are related simply by the equation:

$$L_{sen} = L_{atm} + L_{surf}$$

Therefore, the model atmosphere that has been used to calculate surface radiance must also be able to provide accurate predictions of path radiance. The ability to do this is suspect because path radiance is most dependent on the assumed aerosol model. At this point the aerosol model has been based only on the seasonal average rural aerosol model provided with MODTRAN3. Comparison of observed path radiance with model predictions will be useful at this point. The view geometry of the MODTRAN3 atmosphere corresponding to the time of the blue tarp observation (19.11 hours UT) was changed to produce a radiance spectrum in the zenith direction. The MIE scattering parameter was used in this calculation. The resulting spectrum is compared with the corresponding PGAMS observation in Figure 6. The systematic difference in the two spectra indicate that the model aerosol used does not agree well with the actual atmospheric aerosol properties. Aerosol properties such as single scattering albedo and single scattering phase function that better represents the genuine Sept. 7, 1996 atmospheric aerosols must be evaluated from sky path radiance observations if improved at-sensor radiances are to be predicted from the MODTRAN3 model.

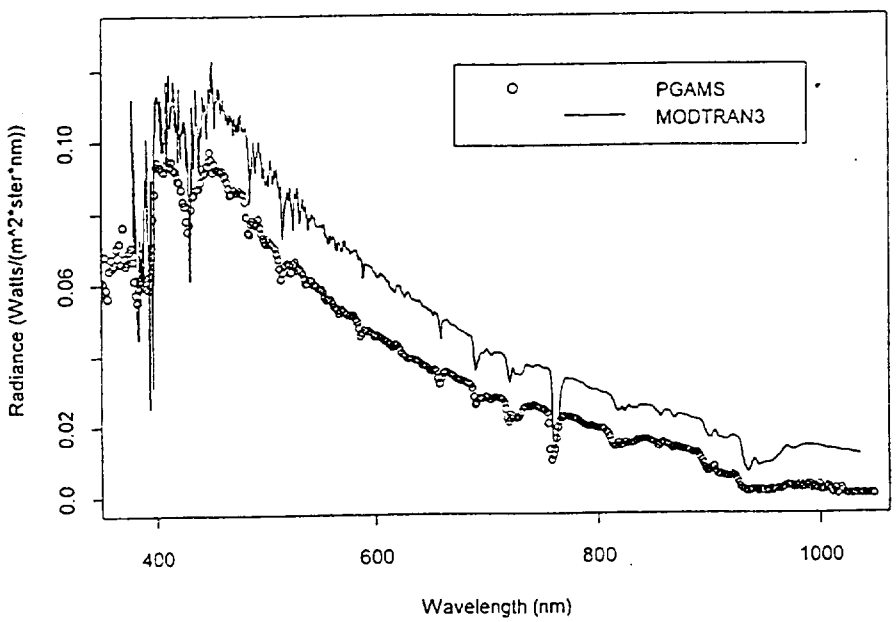

Figure 6. Comparison of the sky path radiance in the zenith direction between an observed PGAMS spectrum (1° FOV) and a MODTRAN3 spectrum calibrated to the visibility and solar geometry at occurring at 19.11 hours UT.

6. CONCLUSION

Presented in this paper are the results of comparing hyperspectral surface radiances calculated using MODTRAN3 with PGAMS field measurements for a blue tarp and a grass surface target. Very good agreement is obtained by constraining a rural atmospheric model with a calibrated visibility and surface reflectance from PGAMS observations. Reliable

transformation to at-sensor radiances require additional constraints to reflect the actual real-time aerosol properties such as the single scattering albedo and the scattering phase function. Comparison of MODTRAN3 predicted at-sensor radiances with actual radiances observed from the Airborne Thermal/Visible Land Application Sensor (ATLAS) will be presented in a future publication.

7. ACKNOWLEDGMENTS

Acknowledgment is made of support for this research by the NASA/University JOint VEnture (JOVE) in Space Research and the South Dakota Space Grant Consortium. Additional support was provided by the National Science Foundation under Grant #OSR-9452894 and by the South Dakota Future Fund. Acknowledgment is also made for supporting the development of PGAMS by the Marshall Space Flight Center Director's Discretionary Fund.

8. REFERENCES

1. Schiller, S. and J. Luvall, "A portable ground-based atmospheric monitoring system (PGAMS) for the calibration and validation of atmospheric correction algorithms applied to satellite images", SPIE, vol. 2231, pp 191-198, 1994.

2. Berk, A., L.S. Berstein, and D.C. Robertson, "MODTRAN: A moderate resolution model for LOWTRAN 7", Final report, GL-TR-0122, AFGL, Hanscomb AFB, MA, 42 pp., 1989.

3. Anderson, G.P., J.H. Chetwynd, J.-M. Theriault, P. Acharya, A. Berk, D.C. Robertson, F.X. Kneizys, M.L. Hoke, L.W. Abreu, and E.P. Shettle, "MODTRAN2: Suitability for Remote Sensing", Proc. Workshop on Atmospheric Correction of Landsat Imagery, Publ. by Geodynamics Corporation, pp. 65-69, 1993.

4. Markham, B.L., D.L. Williams, J.R. Schafer, F. Wood, and M.S. Kim,"Radiometric Characterization of Diode-Array Field Spectrometers", Remote Sens. Environ., vol. 51, pp. 317-330, 1994.

Evaluation of the Aerosol Scattering Phase Function from PGAMS Observation of Sky Path Radiance

Stephen Schiller
South Dakota State University
Physics Department, Brookings, SD 57007
P:605-688-5859/F:605-688-5878/Schilles@mg.sdstate.edu

Jeffery Luvall
Global Hydrology & Climate Center
NASA, Marshall Space Flight Center
977 Explorer Blvd., Huntsville, AL 35806
P:205-922-5886/F:205-922-5723/jluvall@msfc.nasa.gov

Abstract -- A knowledge of the spectral and geometrical distribution of sky path radiance at the time a remote sensing image of the earth's surface is acquired can greatly improve the application of atmospheric correction and vicarious calibration techniques. The focus of this investigation is to evaluate the sensitivity of the radiance exiting the bottom and top of the atmosphere to the representation of the aerosol single-scattering phase function for these applications. Hyperspectral almucantar sky path radiance measurements obtained with the Portable Ground-based Atmospheric Monitoring System (PGAMS) are compared to synthetic spectra generated by MODTRAN3.

INTRODUCTION

The objective in applying atmospheric corrections to remote sensing images is to transform at-sensor radiance to surface radiance and reflectance. The results of the transformation depend largely on the ability to estimate the radiance contribution produced by solar radiation scattered into the sensor's field of view by atmospheric aerosols. The accuracy one can achieve in estimating this path radiance component depends on the representation used for the aerosol single scattering phase function [1].

Typically the approach to developing a single scattering phase function is based upon seasonal average aerosol properties. Using these properties to define a particle size distribution and complex index of refraction, the phase function may be constructed by Mie theory [2]. Another effective tactic is achieved by adopting an asymmetry factor and employing the Henyey-Greenstein phase function [3]. Once generated, the single scattering phase function can be used in radiative transfer calculations to estimate the at-sensor path radiance contribution needed for atmospheric corrections routines.

The Moderate Resolution Atmospheric Radiance and Transmittance Model MODTRAN3 [4] encompasses both of these approaches in generating the aerosol single-scattering phase function and provides a very flexible and powerful platform for sky path radiance calculations. The capacity to deal with the complex problems of multiple scattering makes this code an excellent tool for generating synthetic spectra that can be compared to field observations. In this investigation, comparison will be made to hyperspectral observations obtained with the Portable Ground-based Atmospheric Monitoring System (PGAMS) [5]. The aim of this present work is to evaluate the sensitivity of the adopted aerosol single-scattering phase function in reproducing sky path radiance spectra obtained at different scattering angles.

OBSERVATIONS

The sky path radiance observations were collected using PGAMS in support of a field campaign dealing with the analysis of urban heat island development over Huntsville, Alabama on September 7, 1994. PGAMS obtains radiometric measurements using a Personal Spectrometer (PS) 2 diode-array field spectrometer built by Analytical Spectral Devices [6]. This instrument covers a range of 350 nm to 1050 nm, sampling in 1.4 nm steps, producing a linear response over a dynamic range greater than 3000:1.

A 1° field-of-view end-receptor is mounted on an alt-alt tracking system furnishing input to the spectrometer through a fiber optic bundle. Once set up in the field, the tracking system is calibrated to provide altitude and azimuth pointing of the end-receptor to an absolute accuracy, over the hemisphere of the sky, of better than 1°. Radiometric calibration of the end- receptor/spectrograph combination is made using a LI-COR optical radiation calibration unit. A NIST secondary standard lamp is used for absolute radiance calibration delivering an accuracy of better than 5% over the wavelength range of the spectrometer.

For this investigation, PGAMS recorded both direct solar irradiance and sky path radiance observations. The direct solar irradiance data was used in standard Langley plot analysis to monitor atmospheric transmittance and aerosol optical depth

0-7803-3068-4/96$5.00©1996 IEEE

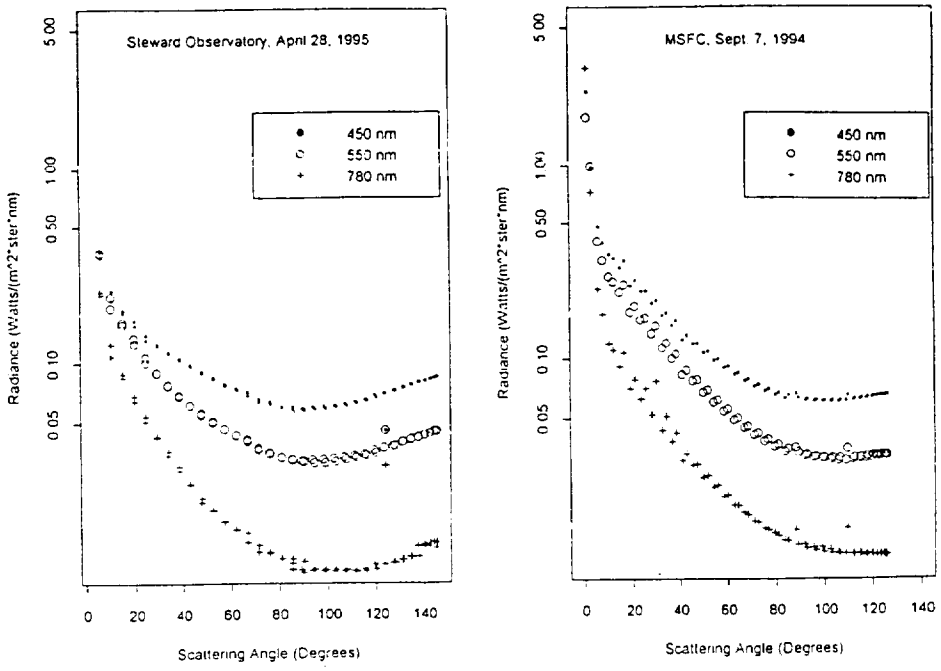

Fig. 1. Almucantar scans recorded at Steward Observatory, Arizona and Marshall Space Flight Center, Huntsville, Alabama. The scans were made at the sun's altitude of 15° and 27° respectively. Only the data for 3 of the 512 PGAMS channels are shown.

over visible and near-infrared wavelengths unaffected by the water vapor bands. The sky path radiance observations consisted of constant altitude scans with 5 degree azimuth steps over a full 360 degree azimuth circle. This resulted in a constant air mass data set in which the dominant radiance variation is due to changes in the "atmospheric" scattering phase function, the integrated scattering phase function from Rayleigh and aerosol single and multiple scattering processes. Fig. 1 presents scans obtained at the sun's altitude at two sites with significantly different aerosol loading. Note that a 360° azimuth scan records the phase function twice. Differences reflect variations in sky conditions and changes in the optical depth of the sun during the observation interval.

ANALYSIS AND DISCUSSION

Synthetic spectra were generated using MODTRAN3 for the purpose of trying to reproduce the observed "atmospheric" phase function and path radiance spectra focusing on the effects of the selected aerosol single scattering phase function. The data set recorded at MSFC, Huntsville, Alabama was employed. Calibration of MODTRAN3 to reflect the actual atmospheric conditions was done by using observations of direct solar irradiance obtained just a few minutes before the constant altitude scan. The sun photometry provided direct measurement of atmospheric transmittance. This was replicated with MODTRAN3 by selecting a spring/summer rural aerosol model and adjusting the visibility until the difference between the observed and synthetic spectra was minimized for wavelengths outside atmospheric water bands. The resulting fit is presented in Fig. 2. The MODTRAN spectrum is based on a solar zenith angle of 62.1° and a visibility of 48.0 km using the 1976 standard atmosphere. The excellent agreement may lead one to expect that accurate path radiance spectra would also result from this model.

Path radiance spectra were calculated with MODTRAN3 to generate an atmospheric scattering phase function for comparison. The initial results employed the aerosol single-scattering phase function based on Mie theory calculations. Because PGAMS was set up at a site dominated by large grassy fields, the vegetation a grass surface albedo was selected along with the 2 stream multiple scattering option. The slant path and solar zenith angles were set at 63° to match the observations and the path radiance was calculated over a range of azimuthal angles between 2° and 180°. The resulting phase function is presented in Fig 3 for wavelengths of 450 nm, 550 nm, and 780 nm. Good agreement is revealed at small scattering angles but in the back scattering realm large systematic differences are revealed.

Making use of the Henyey-Greenstein phase function instead of the fixed MIE scattering rural aerosol model can significantly improve the fit at large scattering angles by adjusting the asymmetry factor. Fig 3. shows the resulting phase function based on asymmetry factors of 0.70, 0.68, and 0.72 at the wavelengths of 450 nm, 550 nm, and 780 nm respectively. Corresponding surface albedos of 0.06, 0.09, and 0.20 were .

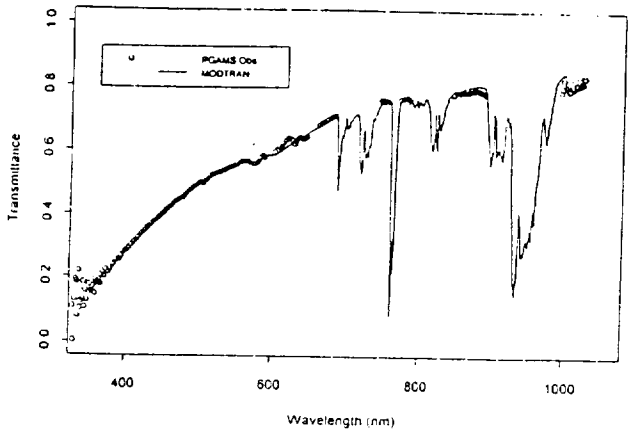

Fig. 2. MODTRAN3 fit to PGAMS transmittance spectra based on a solar zenith angle of 62.1° and a visibility of 48.0 km.

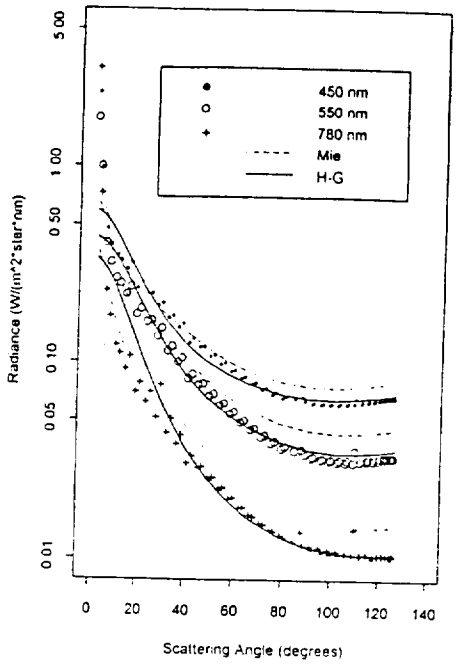

Fig. 3. PGAMS observed "atmospheric" scattering phase function compared to MODTRAN3 path radiance calculations for Mie and adjusted Henyey-Greenstein phase functions.

also utilized.

The improvements made at large scattering angles from the adjustments to the MODTRAN3 model based on fitting the observed phase function is shown in Fig. 4. This is a PGAMS path radiance spectrum recorded at a scattering angle of 120° along with the corresponding MODTRAN3 Mie and Henyey-Greenstein calculations. Even with hyperspectral sun photometry the Mie bottom of the atmosphere calculations are in error by 20 to 30%. Significantly less error is obtained with the adjusted Henyey-Greenstein calculations when the observed atmospheric phase function is also considered. This improvement in bottom of the atmosphere radiance calculations should also be reflect in the calculation of the top of the atmosphere radiances and the application of atmospheric corrections in remote sensing.

CONCLUSION

MODTRAN3 is a highly sophisticated radiative transfer code that is representative of the most effective models used for atmospheric correction and vicarious calibration applications in remote sensing. The results of this investigation reveal, even with such powerful codes, that path radiance spectra over a range of scattering angles from *in situ* observations are critical in accurately calculating radiances exiting the bottom and top of the atmosphere. This originates primarily from the sensitivity of the exiting radiances to the selected aerosol single-scattering phase function which can vary greatly, on a given day, from the seasonal average.

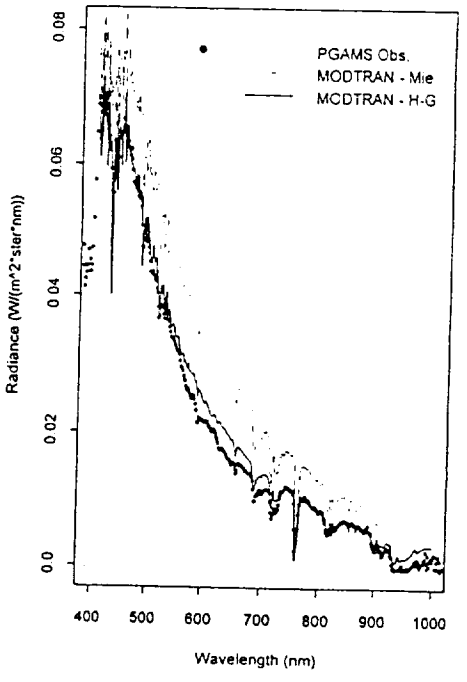

Fig. 4 PGAMS Sky path radiance spectra compared to MODTRAN3 spectra based on the Mie calculated single-scattering phase function for rural aerosols and the adjusted Henyey-Greenstein phase function (see text). The scattering angle is 120°

ACKNOWLEDGMENTS

S..S. would like to acknowledge support provided by the NASA/University JOint VEnture (JOVE) in Space Research and the South Dakota Space Grant Consortium. Additional support was provided by the National Science Foundation under Grant #OSR-9452894 and by the South Dakota Future Fund.. Acknowledgment is also made by J.L. and S.S. for supporting the development of PGAMS by the Marshall Space Flight Center Director's Discretionary Fund.

REFERENCES

[1] M.A. Box and C. Sendra,"Sensitivity of Exiting Radiances to Details of the Scattering Phase Function," J. Quant. Spectrosc. Radiat. Transfer, vol. 54, pp. 695-703, 1995.

[2] K.N. Liou, *An Introduction to Atmospheric Radiation,* Academic Press, New York, 1980.

[3] L.G. Henyey and J.L. Greenstein, "Diffuse Radiation in the Galaxy," Astrophys. J., vol.93, pp. 70-83, 1941.

[4] G.P. Anderson, et al., "MODTRAN3: Suitability as a Flux-Divergence Code", Proceedings of the Fourth Atmospheric Radiation Measurement (ARM) Science Team Meeting, Charleston, South Carolina, CONF-940277, pp. 75-80, April 1995.

[5] S. Schiller, and J. Luvall, "A portable ground-based atmospheric monitoring system (PGAMS) for the calibration and validation of atmospheric correction algorithms applied to satellite images,"SPIE, vol. 2231, pp. 191-198, 1994.

[6] B.L. Markham, D.L. Williams, J.R. Schafer, F. Wood, and M.S. Kim,"Radiometric Characterization of Diode-Array Field Spectroradiometers," Remote Sens. Environ., vol. 51, pp. 317-330, 1995.

Dennis Helder South Dakota State University Nov 21, 1997

I. Research

Brief summary of research results to date on your project:

My initial research project involved developing quality metrics for satellite image data that had been compressed. However, after about a year into the program, it became clear that more progress could be made and support found by addressing satellite radiometry issues, specifically those presented by the Landsat 7 project. As a result of this change in focus, most of my work has been conducted in conjunction with Dr. John Barker, Code 925, Goddard Space Flight Center. We have been characterizing the Landsat 4 and 5 Thematic Mappers radiometric properties at three time intervals: within and orbit; over an outgassing cycle (30-90 days); and over the lifetime of the instruments. We have discovered that the sensor response varies with temperature even within an orbit. This is thought to be due to temperature change of the primary focal plane, and is not observed with detectors in the cold focal plane. Within an outgassing cycle, the only detectable changes occur in the cold focal plane. The response of these detectors is due to build-up of ice or other foreign material on the dewar face. Over the lifetime of the instrument several changes have been observed and are still under investigation. An initial decay in detector response occurred during the first year of orbit which is thought to be due to outgassing of the spectral filters. After this point in time, two of three calibration lamps exhibit catastrophe changes in their radiance levels. Additionally, there are long term changes (both increases and decreases) in detector response that are possibly due to lamp changes, detector changes, or both. These issues remain to be sorted out and hopefully some preliminary results can be reported in the few months.

In addition to this project, we have been working on another project to determine the impact that radiometric and geometric calibration has on typical applications of satellite image data. This project began a few months ago and we have concentrated on developing algorithms and acquiring appropriate test data sets. To assess the impact of radiometry on image applications we have developed a process to produce nearly 'perfect' data from Landsat 5 images based on the Landsat 7 Image Assessment System. From these data sets, we have developed techniques to precisely degrade the imagery with a known radiometric error. We are currently in the process of assessing the initial impact of these degradations on image classification applications. We have noted the nearly 'perfect' data produces significantly better clustering results in the classification process.

A third, and entirely unrelated, research project to develop ethanol as an alternative fuel for general aviation aircraft has been sponsored without NASA support but certainly falls within NASA's general areas of interest. Pursuant to this project we have developed a new form of ethanol-based fuel that overcomes pure ethanol's deficiencies in mixture balance and cold starting capability. This fuel has been used successfully in a carburated aircraft that is undergoing flight testing with the FAA for acquisition of a supplemental type certificate.

Where do you see your JOVE Research going after the initial JOVE funding expires?

Fortunately, I have developed a line of support through the Landsat Project Science Office (Dr. Darrel Williams) at Goddard Space Flight Center. Additionally, I have a proposal funded as a co-investigator on the Landsat 7 Science Team. I believe these opportunities will continue for the next several years.

Communication with NASA Colleague

Initially, I was working with Mr. Les Thompson, Code 975, at Goddard Space Flight Center. After about a year of interaction, it became apparent that a greater opportunity was available through working with Dr. John Barker, Code 925, Goddard Space Flight Center. Dr. Barker and I communicate on a regular basis in a very productive manner. His experience and insight into the operation of Landsat sensors has been tremendously beneficial in guiding my research into the radiometric of these instruments. I believe the match has been beneficial to both of us and I suspect we will continue collaborating for the next several years.

Refereed Journal Articles Published:

LANDSAT TM MEMORY EFFECT CHARACTERIZATION AND CORRECTION,

Dennis Helder	Wayne Boncyk	Ron Morfitt
South Dakota State University	EROS Data Center	EROS Data Center

invited paper, Canadian Journal of Remote Sensing, accepted for publication in the January, 1998 issue

Refereed Journal Articles Submitted

AN ADAPTIVE DEBANDING FILTER FOR THEMATIC MAPPER IMAGES,

Dennis Helder	Joy Hood	Daniel Krause
South Dakota State University	EROS Data Center	North Dakota State University

IEEE Transactions on Geoscience and Remote Sensing, in review

Oral and Poster Papers Presented:

A Radiometric Calibration Archive for Landsat TM, D.L. Helder, Algorithms for Multispectral and Hyperspectral Imagery II, Volume 2758, pp. 273-284, SPIE, April 9-11, 1996, Orlando, FL.

Short Term Calibration of Landsat TM: Recent Findings and Suggested Techniques, D.L. Helder, W. Boncyk, J.L. Barker and B.L. Markham, IGARSS '96, May 27-31, 1996, Lincoln, NB, pp. 1276-1278.

Artifact Corrrection and Absolute Radiometric Calibration Techniques Employed in the Landsat 7 Image Assessment System, Boncyk, W.C., B.L. Markham, J.L. Barker, D.L. Helder, IGARSS '96, May 27-31, 1996, Lincoln, NB, pp1270-1272.

Landsat-7 Enhanced Thematic Mapper Plus In-Flight Radiometric Calibration, Markham, B.L., J.L. Barker, W.C. Boncyk, E. Kaita, D.L. Helder, IGARSS '96, May 27-31, 1996, Lincoln, NB, pp. 1273-1275.

Independent Grant Activity

"Landsat TM Calibration Study", NASA, November 1996 - 1999, NAG5-3540, $182,502
"Characterization of Landsat 7 Geometry and Radiometry for Land Cover Analyses", NASA, November 1996-1999, NAG5-3445, $241,224
"Imaging and Modeling of Coupled Environmental Processes," NSF EPSCoR, 1995-8, $944,109
"Certification and Operational Development of an Ethanol Powered Aircraft", SD Corn Utilization Council, July 1, 1996 -- July 1, 1999, $159,416
for all three projects the primary use of funds is to provide release time for me and student support...

Are you utilizing the Internet or other network?

Internet usage occurs on a daily basis with e-mail, ftp, and web-browsers.

Please identify the data sets, if any used in your research.

Extensive usage has been made of Landsat 4,5 Thematic Mapper data, over 600 scenes. ASAS data has also been used, including one overflight of our target at Brookings, SD, last August, 1997.

II. Education

Assessment of Student Impact.....

Attached to this report are enrollment numbers for the SDSU College of Engineering from 1989 to the present. JOVE investigators are in the Engineering Physics (Steve Schiller) and Electrical Engineering (Dennis Helder) departments. The changes noted in the attachment are more likely due to nationwide trends in engineering enrollment than any other single factor.

Student Research Assistants

Undergraduates Assistants	Research Area	Major
Brian Enga	Data compression	EE
Terrance Boon	Computer support	EE
Melanie Erickson	Satellite Radiometry	EE
Adam Fausch	Satellite Radiometry	EE
Rick Vreeland	Satellite Radiometry	EE
Graduate Assistants:		
Kun Yang	Data Compression	EE

III. Curriculum Development

New Curricula -- none

New Courses:
EE 693 Special Topics in Advance Digital Image Processing

Amended or Augmented Courses:
EE 475/575 Digital Image Processing

IV. Outreach

DeSmet High School Career Day (1993-97) discussion of engineering as a career choice	DeSmet, SD	50 each year
South Dakota Space Day 1995-97	Rapid City, Pierre, Sioux Falls	2000 each year

V. Summer Programs:

VI. "Roadblocks to Progress

The most critical aspect of the program is to select the correct NASA mentor. If you can find someone who is not 'too busy' and can see the advantages of leveraging program resources with a JOVE association, your chances for success are greatly increased. So, perhaps an area for improvement (or roadblock removing) would be to spend some time and effort up front finding that optimal mentor to work with. Would it be possible for the JOVE faculty member to spend some time at a NASA center before the summer experience to insure that the right mentor is selected? Also, is it possible to better educate potential NASA mentors of the benefits of using a JOVE person in their programs? If the long term (3+ years) potential can be demonstrated to NASA personnel, I think the potential for a successful JOVE experience, along with follow-on funding/interaction, will be enhanced.

VII. How could the program be changed to make it more effective?

See above.

VIII. Overall, what has been your institution's greatest benefit from participating in JOVE?

The institution has benefited greatly by increased ties with NASA. This has allowed a significant increase in research grants (Landsat 7 Science team), outreach programs (Space Grant), and faculty opportunities (Summer Fellowships)

IX. Please list all subject inventions as a result of this award or provide a statement that there were none.
NONE.

March 14, 1996

1996 NASA/UNIVERSITY JOINT VENTURE -- STUDENT INFORMATION

Name of JOVE Student Researcher: Rick Vreeland

Social Security Number: [redacted]

Permanent Mailing Address: 1309 Harriet Ave
Carroll Iowa 51401

Permanent Telephone Number: 712-792-5180

School Mailing Address: 204 B Folsom St
Brookings SD 57006

School Telephone Number: 605-697-5294

JOVE Faculty Advisor: Dr Helder

Undergraduate Institution: South Dakota State University

Expected Graduation Date: December 98

Degree Expected: BS in Electrical Engineering

Department: Electrical Engineering

Major declared as a freshman: Electrical Engineering

Do you plan to obtain an advanced degree? If so, where will you obtain it from? Yes, possibly Purdue

Has the JOVE program affected your future plans? If so how? Yes, it has given me an insight into the Field of Image Processing.

In order to determine the degree to which members of the diverse segments of the population are involved in this program, we request that you fill in the appropriate blocks. Completion of this part is voluntary.

X Male ____ Female US Citizenship

Racial Minority: X No ____ Yes (If yes, please check below.)

____ American Indian or Alaskan Native ____ Black (African American/non-Hispanic)

____ Asian or Pacific Islander ____ Chicano (Mexican-American)

____ White, non-Hispanic origin ____ Other Hispanic origin

March 14, 1996

1996 NASA/UNIVERSITY JOINT VENTURE -- STUDENT INFORMATION

Name of JOVE Student Researcher: Adam Fausch

Social Security Number: [redacted]

Permanent Mailing Address: 7217 NW 85th Place
Johnston IA 50131

Permanent Telephone Number: (515) 270-6039

School Mailing Address: 204 Folsom B
Brookings SD 57006

School Telephone Number: (605) 697-5294

JOVE Faculty Advisor: Dr. Helder

Undergraduate Institution: South Dakota State University

Expected Graduation Date: May 1998

Degree Expected: EE

Department: Engineering

Major declared as a freshman: EE

Do you plan to obtain an advanced degree? If so, where will you obtain it from? not at this point

Has the JOVE program affected your future plans? If so how? it has shown me a softer side of EE that I still might consider pursueing

In order to determine the degree to which members of the diverse segments of the population are involved in this program, we request that you fill in the appropriate blocks. Completion of this part is voluntary.

X Male	Female	X Citizenship
Racial Minority:	X No	Yes (If yes, please check below.)
American Indian or Alaskan Native		Black (African American/non-Hispanic)
Asian or Pacific Islander		Chicano (Mexican-American)
X White, non-Hispanic origin		Other Hispanic origin

March 14, 1996

1996 NASA/UNIVERSITY JOINT VENTURE -- STUDENT INFORMATION

Name of JOVE Student Researcher: Melanie Erickson

Social Security Number: _____

Permanent Mailing Address: Unknown - went to U. of Missouri

_____

_____

Permanent Telephone Number: _____

School Mailing Address: _____

_____

_____

School Telephone Number: _____

JOVE Faculty Advisor: _____

Undergraduate Institution: _____

Expected Graduation Date: May 99

Degree Expected: _____

Department: _____

Major declared as a freshman: _____

Do you plan to obtain an advanced degree? If so, where will you obtain it from? _____

_____

Has the JOVE program affected your future plans? If so how? _____

_____

_____

In order to determine the degree to which members of the diverse segments of the population are involved in this program, we request that you fill in the appropriate blocks. Completion of this part is voluntary.

_____ Male _____ Female _____ Citizenship

Racial Minority: _____ No _____ Yes (If yes, please check below.)

_____ American Indian or Alaskan Native _____ Black (African American/non-Hispanic)

_____ Asian or Pacific Islander _____ Chicano (Mexican-American)

_____ White, non-Hispanic origin _____ Other Hispanic origin

March 14, 1996

1996 NASA/UNIVERSITY JOINT VENTURE -- STUDENT INFORMATION

Name of JOVE Student Researcher: Kun Yang

Social Security Number: _____

Permanent Mailing Address: Unknown

Permanent Telephone Number: _____

School Mailing Address: _____

School Telephone Number: _____

JOVE Faculty Advisor: _____

Undergraduate Institution: _____

Expected Graduation Date: Graduated Feb 1995

Degree Expected: _____

Department: _____

Major declared as a freshman: _____

Do you plan to obtain an advanced degree? If so, where will you obtain it from? _____

Has the JOVE program affected your future plans? If so how? _____

In order to determine the degree to which members of the diverse segments of the population are involved in this program, we reques that you fill in the appropriate blocks. Completion of this part is voluntary.

✓ Male _____ Female China Citizenship

Racial Minority: _____ No _____ Yes (If yes, please check below.)

_____ American Indian or Alaskan Native

✓ Asian or Pacific Islander

_____ White, non-Hispanic origin

_____ Black (African American/non-Hispanic)

_____ Chicano (Mexican-American)

_____ Other Hispanic origin

March 14, 1996

1996 NASA/UNIVERSITY JOINT VENTURE -- STUDENT INFORMATION

Name of JOVE Student Researcher: Brian Enga

Social Security Number: _____

Permanent Mailing Address: Unknown

Permanent Telephone Number: _____

School Mailing Address: _____

School Telephone Number: _____

JOVE Faculty Advisor: _____

Undergraduate Institution: _____

Expected Graduation Date: Graduated May 1995

Degree Expected: _____

Department: _____

Major declared as a freshman: _____

Do you plan to obtain an advanced degree? If so, where will you obtain it from? _____

Has the JOVE program affected your future plans? If so how? _____

In order to determine the degree to which members of the diverse segments of the population are involved in this program, we request that you fill in the appropriate blocks. Completion of this part is voluntary.

✓ Male _____ Female US Citizenship

Racial Minority: ✓ No _____ Yes (If yes, please check below.)

_____ American Indian or Alaskan Native

_____ Asian or Pacific Islander

_____ White, non-Hispanic origin

_____ Black (African American/non-Hispanic)

_____ Chicano (Mexican-American)

_____ Other Hispanic origin

March 14, 1996

1996 NASA/UNIVERSITY JOINT VENTURE -- STUDENT INFORMATION

Name of JOVE Student Researcher: Terrance Boon

Social Security Number: _____

Permanent Mailing Address: Unknown

Permanent Telephone Number: _____

School Mailing Address: _____

School Telephone Number: _____

JOVE Faculty Advisor: _____

Undergraduate Institution: _____

Expected Graduation Date: Graduated May 1997

Degree Expected: _____

Department: _____

Major declared as a freshman: _____

Do you plan to obtain an advanced degree? If so, where will you obtain it from? _____

Has the JOVE program affected your future plans? If so how? _____

In order to determine the degree to which members of the diverse segments of the population are involved in this program, we request that you fill in the appropriate blocks. Completion of this part is voluntary.

✓ Male _____ Female US Citizenship

Racial Minority: ✓ No _____ Yes (If yes, please check below.)

_____ American Indian or Alaskan Native _____ Black (African American/non-Hispanic)

_____ Asian or Pacific Islander _____ Chicano (Mexican-American)

_____ White, non-Hispanic origin _____ Other Hispanic origin

Short Term Calibration of Landsat TM: Recent Findings and Suggested Techniques

Dennis Helder
South Dakota State University
PO Box 2220, Brookings, SD 57007
605-688-4184/605-688-5880(fax)/helderd@mg.sdstate.edu

John L. Barker
NASA/GSFC Code 925
Greenbelt, MD 20771

Wayne C. Boncyk
EROS Data Center
Sioux Falls, SD 57198

Brian L. Markham
NASA/GSFC Code 923
Greenbelt, MD 20771

Abstract -- Landsat Thematic Mapper (TM) data has traditionally been radiometrically calibrated on an individual scene basis. While this may be adequate for many applications, particularly single date applications, there are many cases where more advanced techniques are necessary. With emphasis today on global change, multi-temporal analysis is common place. Thus, forms of radiometric calibration are required that discriminate temporal change from changes in instrument response. To address this issue, a project is underway to evaluate TM calibration at several different time scales: short term, intermediate term, and lifetime. This paper will present some of the short term results. Short term is defined as within a single orbit. Continuous swaths of night data have been collected and the individual scenes, along with calibration files, stitched together. Analysis of the calibration files has revealed a number of interesting characteristics about detector gain and bias as well as instrument anomalies such as memory effect and scan correlated shift. Detector bias is a rapidly varying parameter that requires evaluation and correction as frequently as every scan. Detector gain varies significantly within an orbit in the primary focal plane in a predictable manner. Scan correlated shift has been accurately quantified and its effects may easily be removed from the data. Memory effect is in the process of being characterized and an algorithm is being developed to remove it. Line droop has been shown to simply be due to memory effect. Results from these investigations are being used in the development of radiometric correction algorithms for the Landsat 7 Image Assessment System.

TM CALIBRATION ARCHIVE SYSTEM

For more than 10 years, data have been collected from the Thematic Mapper instruments on-board Landsat 4 and 5. Early in the lifetime of these instruments significant efforts were undertaken to ensure that the data were well calibrated radiometrically [1-3]. However, over the passage of time these activities diminished significantly. As a result, the ability to extract information from these data has been reduced. Fortunately, the imagery in the archive is maintained with all of the internal calibration information that was obtained at the time of scene acquisition. These calibration data can be used to characterize the instruments on several different time scales and can be correlated with ground-based calibration campaign results.

To accomplish the goal of extracting pertinent calibration data from the TM archive, the TM Calibration Archive System (TMCAS)was developed [4]. This system consists of the software and hardware necessary to ingest data from 8mm tapes, archive calibration data at several levels, calculate various calibration parameters, and also has tools for plotting and statistical analysis.

Calibration of TM will be analyzed at three different time scales. The shortest time scale considered is a single orbit. The intent here was to understand what changes take place during a cycle where the instrument is turned on, acquires data continuously, and then turned off. At the other extreme, calibration data will be extracted over the lifetime of the instruments. Obviously, this allows determination of any long term trends in detector response. Lastly, an intermediate time period will be analyzed corresponding to the interval required for one outgassing cycle.

Over 600 scenes of TM data will be analyzed during the course of this project. Current efforts has been directed toward analysis of data obtained from contiguous single orbits. The rest of this paper will concentrate on the characterization of well-known TM anomalies, anomalies present in single orbit data, and recommendations for calibration based on these results.

SINGLE ORBIT ANALYSIS

Initial analysis of single orbit data sets from Landsat 5 has revealed several interesting anomalies [4]. Scene content has a significant effect on data recorded during the calibration interval. This can be observed by comparing data acquired during daytime descending orbital passes to data acquired during ascending, night orbital passes. Data collected during night has less variability. Additionally, daytime data has more variability on forward scans than on reverse scans. It is hypothesized that these differences are due to memory effect. Differences based on scan direction also exist in the calibration pulse magnitude recorded by the detectors. This observation is independent of day or night acquisitions and may be due to slight alignment differences in the calibration arm assembly on forward and reverse scans. Differences in calibration

0-7803-3068-4/96$5.00©1996 IEEE

A radiometric calibration archive for Landsat TM

Dennis Helder

Electrical Engineering Department
South Dakota State University
Brookings, SD 57007

ABSTRACT

For more than ten years, Landsat Thematic Mapper (TM) data has been collected of the Earth's surface. Although equipped with an internal calibrator, routine temporal analysis of the instrument's radiometry has not been performed. Recently, a project has been initiated to recover TM radiometric calibration data from the Landsat archive to form a TM calibration archive. This archive consists of calibration data collected at several different time scales: single orbit, instrument lifetime, and an intermediate scale. Analysis of these data is providing insights into how detector response, as well as internal calibrator performance, has changed over time. Initial results are shown that indicate changes in detector gain and characterization of instrument anomalies within a single orbit. Information obtained from this project will allow a more accurate calibration of data that is already in the Landsat archive. Additionally, it will directly impact development of correction algorithms for Landsat 7.
Keywords: radiometry, calibration, Landsat

1. INTRODUCTION

1.1. Problem Statement

For more than 10 years, data have been collected from the Thematic Mapper instruments on-board Landsat 4 and 5. This archive of data represents a tremendous resource available for the study of the Earth. Early in the lifetime of these instruments significant efforts were undertaken to ensure that the data were well calibrated radiometrically.[1-4] However, over the passage of time these activities diminished significantly. As a result, the ability to extract information from these data has been reduced. Fortunately, the imagery in the archive is maintained with all of the internal calibration information that was obtained at the time of scene acquisition. These calibration data can be used to characterize the instruments on several different time scales and can be correlated with ground-based calibration campaign results. The purpose of this research has been to develop a mechanism for extraction of calibration data from the TM archive, analyze these data to characterize the instruments over their lifetimes at several different time scales, correlate these data with past ground-based calibration data.

Work thus far has concentrated on developing a system for routine extraction of calibration information from the Landsat TM archive. Because of the large amount of data that to be analyzed, over 600 scenes, it was critical that a system be developed to extract calibration information and archive the data at several different processing levels. This system was developed over the past two years and tested using both Landsat 4 and 5 data. An initial collection of data for the TM calibration archive has been established.

0-8194-2139-1/96/$6.00

Landsat-7 Enhanced Thematic Mapper Plus In-Flight Radiometric Calibration

Brian L. Markham
Code 923, NASA/GSFC
Greenbelt, MD 20771
(301)286-5240 (Voice)
(301)286-0239 (FAX)
Email: markham@highwire.gsfc.nasa.gov

Wayne C. Boncyk
USGS/ EROS Data Center
Sioux Falls, SD 57198
(605)594-6020 (Voice)
(605)594-6529 (FAX)
Email: boncyk@edcsgw4.cr.usgs.gov

John L. Barker
Code 923, NASA/GSFC
Greenbelt, MD 20771
(301)286-9498 (Voice)
(301)286-0239 (FAX)
Email: jbarker@highwire.gsfc.nasa.gov

Ed Kaita
Science Systems and Applications, Inc
Code 923, NASA/GSFC
Greenbelt, MD 20771
(301) 286-5597 (Voice)
(301) 286-0239 (FAX)
Email: kaita@ltpmail.gsfc.nasa.gov

Dennis L. Helder
Department of Electrical Engineering
South Dakota State University
Brookings, SD 57007
(605)688-4184 (Voice)
(605)688-5880 (FAX)
Email: helderd@mg.sdstate.edu

Abstract-- The Enhanced Thematic Mapper Plus (ETM+) for the Landsat-7 satellite is currently in the assembly and integration stage with the satellite due for launch in 1998. The ETM+ is a derivative of the earlier Thematic Mappers (TM's) flown on Landsats 4 and 5. Chief among changes designed to improve radiometric calibration accuracy is the Full Aperture Solar Calibrator (FASC), a diffuse reflecting plate that can be deployed in front of the ETM+ aperture. With knowledge of the reflectance and illumination geometry of this calibrator, an absolute radiometric calibration of the ETM+ can be performed in flight by reference to the sun. Also incorporated on the ETM+ is a Partial Aperture Solar Calibrator (PASC) which can perform more frequent, but less complete calibrations of the ETM+. These two calibration devices, along with an Internal Calibrator similar to the one on the earlier TM's, constitute the on-board calibration capability. Ground Look calibrations will supplement the on -board measurements.

INTRODUCTION

The Landsat-7 mission is to provide continuity with the 20 year record of Landsat imagery starting in 1972 with Landsat-1 and the Multispectral Scanner (MSS). It provides wide area coverage (~185 km swath) on a 16 day repeat cycle with modestly high (15-60 m depending on band) spatial resolution[1]. The sensor on Landsat-7, the Enhanced Thematic Mapper Plus (ETM+) is similar to the Thematic Mappers on Landsats 4 and 5 and the Enhanced Thematic Mapper built for Landsat 6. This sensor is currently being assembled and integrated at Santa Barbara Remote Sensing (SBRS) under contract to NASA. One of the requirements of the Landsat-7 mission is radiometric calibration of the ETM+ data to an uncertainty of less than 5% in at-aperture radiance. This requirement, which is more stringent than in the past for the Landsat program, is being met by some improvements in the design and new calibration hardware, e.g., improved bandpass filters and full and partial aperture calibrators, a planned program of ground look calibrations and changes in the radiometric calibration ground processing. This paper addresses the new full aperture calibrator, its pre-launch characterization and in-orbit usage. A companion paper [2] addresses the radiometric processing changes. This paper is an update to [3].

FULL APERTURE SOLAR CALIBRATOR (FASC)

Design

The Full Aperture Solar Calibrator (FASC) is a white painted panel that can be deployed in front of the ETM+ aperture and diffusely reflect solar radiation into the full aperture of the instrument. The active surface of the FASC is painted with the classic formulation of YB71, an inorganic flat white paint

0-7803-3068-4/96$5.00©1996 IEEE

Artifact Correction and Absolute Radiometric Calibration Techniques Employed in the Landsat 7 Image Assessment System

Wayne C. Boncyk
U. S. Geological Survey
EROS Data Center, Sioux Falls, SD 57198
605-594-6020 fax:605-594-6529 boncyk@edcsgw4.cr.usgs.gov

Brian L. Markham
NASA/GSFC
Code 923, Greenbelt, MD 20771
301-286-5240 fax:301-286-1757 markham@highwire.gsfc.nasa.gov

John L. Barker
NASA/GSFC
Code 925, Greenbelt, MD 20771
301-286-9498 fax:301-286-1757 jbarker@highwire.gsfc.nasa.gov

Dennis Helder
South Dakota State University
EERC, Brookings, SD 57007
605-688-4184 fax:605-688-5880 helderd@mg.sdstate.edu

Abstract -- The Landsat-7 Image Assessment System (IAS), part of the Landsat-7 Ground System, will calibrate and evaluate the radiometric and geometric performance of the Enhanced Thematic Mapper Plus (ETM+) instrument. The IAS incorporates new instrument radiometric artifact correction and absolute radiometric calibration techniques which overcome some limitations to calibration accuracy inherent in historical calibration methods. Knowledge of ETM+ instrument characteristics gleaned from analysis of archival Thematic Mapper in-flight data and from ETM+ prelaunch tests allow the determination and quantification of the sources of instrument artifacts. This a priori knowledge will be utilized in IAS algorithms designed to minimize the effects of the noise sources before calibration, in both ETM+ image and calibration data. Gain and Bias estimates for each ETM+ detector that are derived from onboard calibrators are tracked with Ground based measurements, and with prelaunch measurements of instrument gains and biases as part of a Combined Radiometric Model (CRaM), to yield improved estimates of absolute gain and bias per channel. Trends in these instrument parameters are observed and recorded, allowing for the development of analytic models of detector gain and bias as functions of time and instrument state. IAS radiometric calibration methodology, utilizing precalibration artifact correction in conjunction with CRaM gain and bias determination, provides a more consistent absolute calibration of the ETM+ than that possible with historical TM calibration approaches.

0-7803-3068-4/96$5.00©1996 IEEE

HISTORICAL PERSPECTIVE

The Thematic Mapper (TM) instruments flown on Landsats 4 and 5 were designed to provide image data to an overall absolute radiometric calibration accuracy of 10 per cent, and a band to band accuracy of better than 2 per cent [1]. The TM only has one onboard calibration reference source, the Internal Calibrator (IC) comprised of three halogen lamps for reflective band calibration and a heated black body for emissive band calibration. Thus, TM absolute radiometric calibration has been a daunting task. Within-band relative calibration has also proven somewhat difficult, as uncertainties in the position of the IC shutter and in the knowledge of cal pulse intensity as a function of position along the shutter flag have led to errors in the determination of each detector's response to input radiance.

Further complicating TM calibration has been the presence of various sources of instrument, spacecraft and transmission noise that have introduced radiometric "artifacts" such as Scan Correlated Shift (SCS), Memory Effect (ME), and Coherent Noise (CN), amongst others, into TM imagery. These artifacts place further limits on the radiometric quality of TM imagery.

Two approaches have traditionally employed to calibrate TM imagery. The method developed at NASA/GSFC uses a least squares regression technique on data provided from the IC to find a nominal gain and offset for each detector, based on cal data provided with the scene [2]. A variant of this approach has offsets determined scan by scan.

TO: Dennis Heldt

From Barb

COLLEGE OF ENGINEERING
SOUTH DAKOTA STATE UNIVERSITY
Enrollments

	YEAR	AE	CE	CSCI	EE	EET	EAFB	EP	GE	ME	PRE-ARCH	TOTALS	TOTAL WOMEN
First Year	1991	16	62	32	70	13	6	5	73	93	17	387	46
	1990	18	60	20	88	17		2	83	101	12	401	34
	1989	20	39	28	89	14		10	65	102	13	380	30
Second Year	1991	7	39	22	45	13	17	6	18	54	0	221	25
	1990	5	41	13	50	23		1	17	64	1	215	20
	1989	4	34	18	53	21		2	14	46	3	195	19
Third Year	1991	7	40	10	41	21	15	0	10	65	0	209	18
	1990	8	30	13	55	24		1	4	58	0	193	20
	1989	6	40	14	81	30		4	5	50	2	232	25
Fourth Year	1991	8	45	21	84	26	15	4	1	61	0	265	29
	1990	6	51	22	104	28		5	3	70	0	289	35
	1989	7	52	19	93	38		6	2	62	0	279	23
Under Grad Sub-Total	1991	38	186	85	240	73	53	15	102	273	17	1082	118
	1990	37	182	68	297	92		9	107	293	13	1098	109
	1989	37	165	79	316	103		22	86	260	18	1086	97
M. Sc.	1991	9	51	0	25	0	0	13	36	36	0	170	28
	1990	5	31	0	23	0	0	6	31	9	0	105	13
	1989	13	30	0	25	0	0	7	13	11	0	99	7
TOTAL	1991	47	237	85	265	73	53	28	138	309	17	1252	146
	1990	42	213	68	320	92		15	138	302	13	1203	122
	1989	50	195	79	341	103		29	99	271	18	1185	104

This info is gathered in fall of year.

COLLEGE OF ENGINEERING
SOUTH DAKOTA STATE UNIVERSITY
Enrollments

	YEAR	AE	CE	CM	CSCI	EE	EET	EP	Food &Bio	GE	ME	TOTALS	TOTAL WOMEN
First Year	1994	27	99	0	28	80	14	10	0	65	97	420	49
	1993	24	70	0	36	61	24	5	1	63	82	366	45
	1992	24	75	0	38	66	16	8	0	68	85	400	49
Second Year	1994	12	45	2	34	34	24	3	0	14	55	221	25
	1993	19	55	0	19	33	16	4	0	15	50	211	29
	1992	10	45	0	17	35	19	2	0	20	57	221	16
Third Year	1994	11	54	0	19	30	21	4	0	6	59	204	31
	1993	7	46	0	19	35	23	1	1	3	56	191	13
	1992	10	46	0	14	48	14	3	0	4	62	216	19
Fourth Year	1994	8	53	0	21	57	26	5	1	4	87	262	21
	1993	12	51	0	15	63	28	3	0	0	99	271	25
	1992	8	42	0	29	53	22	1	0	7	77	252	29
Under-Grad Total	1994	58	251	2	102	201	85	22	1	89	298	1107	126
	1993	62	222	0	89	192	91	13	2	81	287	1089	112
	1992	52	208	0	98	202	71	14	0	99	281	1089	113
Master of Science	1994	10	51	0	17	35	0	10	0	33	45	201	27
	1993	14	58	0	28	30	0	10	0	44	55	239	25
	1992	11	64	0	12	28	0	8	0	75	55	253	24
TOTAL	1994	68	302	0	119	236	85	32	1	122	343	1310	153
	1993	76	280	0	117	222	91	23	2	125	342	1278	138
	1992	63	272	0	110	230	71	22	0	174	336	1342	137

COLLEGE OF ENGINEERING
SOUTH DAKOTA STATE UNIVERSITY
Enrollments

Revised 11/3/97

	YEAR	AE	CE	CSc	CM	EE	EET	PHYS	*EP	GE	MET	ME	TOTALS	TOTAL WOMEN
First Year	1997	28	54	62	21	64	15	1	2	40	4	81	372	36
	1996	22	84	36	16	45	17		5	45	1	71	342	26
	1995	21	107	33	11	56	13		3	43	0	75	362	39
Second Year	1997	12	60	23	33	25	16	1	4	12	10	54	250	25
	1996	10	63	23	18	28	16		4	10	0	42	214	24
	1995	7	62	29	13	48	15		3	9	0	60	246	34
Third Year	1997	7	48	20	18	28	15	2	2	5	2	40	187	19
	1996	3	47	12	21	36	13		3	1	0	53	189	26
	1995	13	53	28	0	25	24		3	2	0	55	207	28
Fourth Year	1997	6	78	31	15	60	18	4	5	3	4	72	296	36
	1996	16	73	34	7	53	28		2	0	0	75	290	34
	1995	7	63	22	1	43	15		3	0	0	84	240	32
Under-Grad Total	1997	53	240	136	87	177	64	8	13	52	20	247	1105	116
	1996	51	267	114	53	162	74		14	56	1	241	1035	110
	1995	48	285	112	25	172	67		12	54	0	274	1055	133
Master of Science	1997	9	42	28	0	17	0	0	4	38	0	17	155	18
	1996	10	38	36	0	32	0		9	40	0	16	181	36
	1995	10	36	29	0	40	0		7	34	0	30	186	28
TOTAL	1997	62	282	164	87	194	64	8	17	90	20	264	1260	134
	1996	61	305	150	53	194	74		23	96	1	257	1216	146
	1995	58	321	141	29	212	67		19	88	0	304	1241	161

* There are 13 students not included in the count with EP as their second major--6 have a first major of EE & 7 have ME as a first major.

LANDSAT TM MEMORY EFFECT CHARACTERIZATION AND CORRECTION

Dennis Helder	Wayne Boncyk	Ron Morfitt
South Dakota State University	EROS Data Center	EROS Data Center

Summary

Before radiometric calibration of Landsat Thematic Mapper (TM) data can be done accurately, it is necessary to minimize the effects of artifacts present in the data that originate in the instrument's signal processing path. These artifacts have been observed in downlinked image data since shortly after launch of Landsat 4 and 5. However, no comprehensive work has been done to characterize all the artifacts and develop methods for their correction. In this paper, the most problematic artifact is discussed: memory effect (ME). Characterization of this artifact is presented, including the parameters necessary for its correction. In addition, a correction algorithm is described that removes the artifact from TM imagery. It will be shown that this artifact causes significant radiometry errors, but the effect can be removed in a straight forward manner.

Introduction

Since the launch of Landsats 4 and 5, the Thematic Mapper instruments on those platforms have been providing high quality imagery of the Earth's surface. However, soon after launch it became apparent that the radiometric accuracy of the data returned from the sensors was degraded by the presence of several noise signals that manifest themselves as artifacts in resulting TM image products. Although the

impairment from the artifacts is not large, it is, nonetheless, significant. Characterization and removal of these artifacts from TM data should allow users to better extract quantitative information from their imagery and remove resulting errors in application analyses caused by artifacts, such as classification algorithm results that are corrupted by memory effect. Since Landsat 5 is the only TM sensor still actively providing data, only this instrument will be considered here. However, the techniques presented can also be applied successfully to Landsat 4 TM data with appropriate modification of model parameters. To illustrate the artifacts and their removal, an example scene is presented.

After extensive analysis of TM data, it has been determined that three primary radiometric artifacts exist: memory effect (ME), scan-correlated shift (SCS), and coherent noise (CN). Other secondary artifacts have been identified; however, their effects are significantly less and will not be considered here. All three of these artifacts are normally difficult to observe in the data except in fairly homogeneous regions such as water, snow cover, or desert.

ME has been known by various names in the past such as bright target recovery or banding. It produces light and dark bands in resulting imagery. The ME pattern is definitely periodic: the bands are always 16 lines wide, one brighter scan followed by a darker scan. It is most obvious in homogeneous regions following a sudden transition in intensity, such as at a cloud/land boundary. It is not constant within a scan, but dies out with distance from the intensity transition boundary. This artifact can cause significant errors in radiometry, on the order of several digital numbers, or DN (recall that TM is an 8-bit instrument with output values on a scale from 0 to 255), near transitions.

SCS is a sudden change in the bias of the detectors that occurs in the time interval between scans(Metzler and Malila, 1985, Helder, 1996). All detectors change at the same time, but with different amplitudes. The amount of change is typically quite small, on the order of 1 DN or less. Since all detectors change simultaneously, the effect can be seen in the data as bands (sixteen lines wide) that are of slightly different

intensity. The light and dark bands occur randomly, across multiple scans, without significant evidence of periodic structure.

CN is normally the least offensive of the three radiometric artifacts, introducing uncertainties on the order of 0.25 DN or less (Metzler and Malila, 1985). A characterization and correction methodology for CN will not be discussed here.

One of the difficulties inherent in artifact characterization is that normally the artifact amplitude is quite small in comparison with the actual image data, often on the order of less than one DN. Secondly, at least in the case of ME, the artifact is image content dependent. For these two reasons, most of the artifact characterization work has been done using night imagery collected during an ascending orbit. Two data sets were analyzed: December 25, 1984, Path 23 Rows 214-234, and October 21, 1985, Path 116 Rows 199-225. These sets represent the longest contiguous segments of night data available in the EROS Data Center (EDC) TM Archive. Use of multiple scenes greatly increased the amount of data available and, therefore, improved the accuracy of the artifact parameter estimation process. Additionally, it allowed determination of the presence of short term time dependencies (i.e., are these artifacts independent of time, or do they change within an orbit)?

The following discussion focuses on ME. This artifact is the most troublesome of the three and can also produce the largest radiometric errors. A brief review of the literature will be presented followed by characterization of the artifact. More importantly, a correction procedure that removes ME based on a physical model of the phenomenon is presented. Thus, radiometric accuracy is preserved and even enhanced. An example scene will be presented that is corrupted by ME and subsequently restored. The final sections discuss the characterization and summarize implementation of the suggested correction technique.

Background

Memory Effect (ME) has been known by a variety of names, such as "banding," "bright target recovery," "bright target saturation," "scan-to-scan striping," and "radiometric hysteresis," since it was first observed after the launch of Landsat 4 (Barker and Gunther, 1983, Barker, 1983, Murphy, 1986, Srinivasan et al, 1988). ME is commonly observed in imagery that contains large homogeneous regions immediately adjacent to a sharp intensity transition such as a cloud/desert or snow/water boundary that is not parallel to a scan line. System response is depressed after scanning past the transition for an interval of several thousand minor frames. Consider, for example, a water scene consisting of a large cloud bank about 1000 pixels wide on the West side of the image. On a forward scan, as the instrument scans from the clouds onto the water, the detector response is immediately depressed on the order of one to two DN. This effect diminishes as the instrument finishes its forward scan. On the reverse scan, ME has entirely recovered and as the instrument scans toward the cloud bank from the East, the detectors are responding normally and are not depressed. As a result, darker scans are observed in an alternating fashion adjacent to the sharp transition with an intensity difference of up to several DN that decreases with distance from the cloud bank. ME has not been observed in Bands 5, 6 and 7 that reside on the cold focal plane, only TM Bands 1 through 4 are affected. This is due to the difference in design of the preamplifiers for the cold focal plane detectors.

Over the years, several methods have been proposed to remove ME. Most have relied on some type of filtering approach to perform a cosmetic improvement. Fusco et al. (1986) developed a recursive filtering approach along scan lines based on model parameters derived from an analysis of "bright" edges. Although not derived directly from a physical model or data uncorrupted from image content, the approach is closely related to what is presented here and was able to provide reasonable estimates of ME

parameters. Srinivasan et al. (1988) developed a restoration filter based on a power spectrum estimation approach. This technique only provided a cosmetic improvement. Another filtering approach developed by Crippen (1989) was very efficient to implement and consisted of simple averaging operations. Lastly, a Wiener filtering approach was developed by Helder et al. (1992) incorporating an adaptive technique to effectively removed ME from data for cosmetic improvement.

Characterization

The methodology reported here used two approaches for characterization of ME: a model of the analog circuitry between the detector and A/D converters in the TM instrument was developed; and the data produced by the instrument itself were analyzed. Theses analyses were conducted in an independent fashion and produced results that were in strong agreement with each other.

Because the ME artifact has an exponential decay, it was postulated that a possible source for this phenomenon is the analog circuitry connecting the detectors to the A/D converters. The signal path immediately following the detectors is a string of linear amplifiers. The pre-amplifier was singled out as the most likely candidate since it provided the most gain in the system and was also the most complex circuit with several supporting feedback mechanisms to ensure overall circuit stability. The pre-amplifier system was analyzed in an exhaustive block-by-block procedure using the circuit analysis software PSPICE. A feedback circuit in the pre-amplifier was determined to exhibit a transfer function dominated by a resistor/capacitor network with a time constant of 0.01 second. Simulations of the pre-amplifier showed that a step input in voltage (simulating a sharp intensity transition from a bright region to a dark region) produced a voltage output that closely mirrored what is observed in the data produced by the instrument. That is, the output of the pre-amplifier undershoots the desired level, and recovers exponentially with a time constant of 10 milliseconds. This time constant is equivalent to an image-based spatial period of 1040 minor frames (or pixels). Unfortunately, since a characteristic model for the

detectors themselves was unavailable, it was impossible to unambiguously determine the magnitude of the system response from the system's electronic model.

In a parallel analysis, a study of 26 night scenes from the EDC archive was undertaken to extract the ME model parameters directly from the data produced by the instrument. It was desired to use night imagery because the only input to the system is well-defined internal calibrator pulses. Thus, the only output from the system during acquisition of night scenes, other than a relatively constant bias level after SCS removal, is a pulse response from the internal calibrator. One difficulty with this procedure is that a gap exists in all archived data sets between the end of a calibration interval, as shown in Figure 1, and the start of the next scan. In order to account for the gap, the analysis was divided into forward scans and reverse scans. As can be seen from Figure 1, the calibration pulse at the end of forward scans occurs near the end of the calibration interval. Thus, the data obtained during the subsequent reverse scans is most strongly affected by ME. These data were analyzed to obtain initial values of ME magnitude and time constant. However, a better estimate of the magnitude of ME can be obtained from reverse scan calibration data. Here, the calibration pulse occurs early in the calibration interval and the shutter region immediately following the pulse can provide an improved estimate of the magnitude of ME. By combining these two pieces of information, a more accurate estimate of ME parameters can be obtained.

The model for ME is based on a first order linear circuit model and, therefore, has a response, after the pulse has occurred, of the form

$$g(t) = b - ke^{-t/\tau} \qquad (1)$$

where g(t) is the ME pulse response

b is the detector bias, DN

k is the ME magnitude, DN

τ is the ME time constant, in minor frames (mf).

The independent variable, t, can be thought of as discretized units of time or as a spatial increment. A TM pixel is acquired approximately every 10 μs. However, it is more convenient to consider t as a spatial variable with units of pixels (or minor frames, mf). The procedure for determining the ME parameters is illustrated in Figure 2. Figure 2a shows data from a single reverse scan for a detector after bias correction. This is the data recorded shortly after the detector has viewed the brightest calibration pulse. ME is difficult to observe. However, in this example there is a sense that values near the beginning of the scan are somewhat less than values at the end of the scan. If all reverse scans for the given lamp state are averaged together over 26 night scenes in a contiguous interval, the result shown in Figure 2b is obtained. Here it is obvious that a depression in detector response exists immediately after the calibration pulse is observed, followed by an increase in an exponential fashion to a constant bias level. However, the data are still quite noisy. Figure 2c show an exponential model fitted to the data after it has been smoothed with a moving average filter. Model parameters are given in Table 1.

An examination of Table 1 reveals that the magnitude of ME is strongest in Bands 2 and 3. Band 2 has a slightly larger average ME amplitude, but Band 3 exhibits larger variability. Band 4 exhibits less ME magnitude, while Band 1 is the least affected of the four. It is also interesting to note that the time constant is fairly consistent in Bands 2, 3, and 4. The Band 1 average time constant is significantly higher. This may simply be due to the fact that Band 1 exhibits the least amount of ME and is, therefore, the most difficult band to estimate ME parameters for. The fact that Bands 2, 3, and 4 are consistent is expected since the assumed cause of ME is the feedback circuit mentioned previously. This circuit design is fundamentally the same for all bands. However, when the circuits were built, gain resistors were carefully matched to individual detectors. Thus, the specific circuitry is slightly different for each detector. This, coupled with inevitable stray capacitances, gives rise to variations in the time constant.

A potential error source exists for the ME parameter estimation method. This technique analyzes data obtained right at the edge of the dynamic range of the detectors. In fact, ME actually causes a depression below the normal detector bias level. As a result, system linearity cannot be guaranteed. This is especially true in observations of data from Band 4. Initial ME magnitude value estimates were low due to this effect. The values presented in Table 1 were adjusted slightly to provide improved ME correction. An explanation of the correction procedure based on these parameters is given in the next section.

Correction

ME is caused by the presence of a resistor/capacitor combination in the electronic pre-amplifier immediately following the detectors. As such, it is modeled as a first order linear system. The output of such a system is obtained by convolving the input signal and the impulse response of the system (Poularikas and Seely, 1985). The impulse response of the system can be derived from the calibration pulse response discussed in the preceding section. Subsequently, a restoration filter can be derived from knowledge of the impulse response of the system. The most direct approach is to simply apply an inverse filter. This can be done successfully only if the transfer function of the system (the Fourier transform of the impulse response) contains no zeros. Fortunately, this is the case for ME and the details are shown below.

The impulse response due to ME has the following form:

$$h_{ME}(t) = A\delta(t) + k_{ME}e^{-t/\tau}u(t) \qquad (2)$$

where k_{ME} is the magnitude of the ME impulse response, τ is its time constant, and u(t) is the unit step function. Parameter 'A' is introduced to insure that no change in steady state bias occurs due to ME, thus $A = 1 - k_{ME}\,\tau_{ME}$. The first term represents the response of the system without ME, while the second term

is the error due to ME. The response of a first order linear system to a square pulse occurring at t = 0, of width T and height P is given as

$$Pk_{ME}\tau(1-e^{\frac{T}{\tau}})e^{\frac{-t}{\tau_{ME}}} \qquad t > T \qquad (3)$$

By equating this expression to (1) above, it can be immediately seen that the magnitude and time constant of the ME impulse response can be obtained from the calibration pulse response as

$$\tau_{ME} = \tau \qquad (4a)$$

$$k_{ME} = \frac{k}{P\tau_{ME}(1-e^{\frac{T}{\tau_{ME}}})} \qquad (4b)$$

Unfortunately, calibration pulses are not perfectly square with width T and height P. However, a reasonable approximation can be obtained. The width of the pulse, T, is assumed to be the distance in minor frames (mf), or sample values, between the locations on the skirts of the pulse that have values 10% of the peak value of the pulse. Average pulse height, as calculated by integrating over this range of pulse values and dividing by the number of mf, can be used for P. Average calibration pulse height values for Bands 1 to 4 are given in Table 2 for lamp state [111] where all lamps are on. Pulse widths are 50 mf for all bands.

With knowledge of the form of the ME impulse response and estimates of the calibration pulse, as well as the output from a calibration pulse, the ME impulse response parameters can be obtained without a deconvolution operation or use of Fourier transformation. The form of the impulse response is exponential and therefore of infinite duration. However, from a practical point of view, a limited duration

approximation on the order of 3000 mf is reasonable. Past this point the system response to ME is far smaller than the quantization level and unmeasurable.

Once the impulse response for ME has been obtained, a restoration filter can be developed. Many approaches are available for deriving restoration filters. The simplest of these, inverse filtering, is applicable here. This can be shown in the following way. Consider the system model below

$$y(t) = h(t) * x(t) + n(t) \qquad (5)$$

where convolution is denoted by *, y(t) is the observed signal or image, x(t) is the desired signal or image, h(t) is the transfer function of the system, and n(t) represents a noise process usually modeled as additive zero-mean, white noise. This expression has the well-known analogous form following Fourier transformation,

$$Y(\omega) = H(\omega)X(\omega) + N(\omega). \qquad (6)$$

where ω is spatial frequency. The inverse filtering approach uses the restoration filter $W(\omega) = 1/H(\omega)$ to obtain an estimate of $X(\omega)$

$$\hat{X}(\omega) = Y(\omega)W(\omega) = \frac{Y(\omega)}{H(\omega)} = X(\omega) + \frac{N(\omega)}{H(\omega)}. \qquad (7)$$

This method works well if no noise is present in the system. Under this condition, the second term in the above expression disappears and perfect restoration is possible. However, with ME this is certainly not the case as Figure 2 readily shows. Normally, noise is present and, if it is white, it has a constant power spectrum. Under these conditions the second term does not disappear. However, its effects can be

minimized if $|H(\omega)| > 1$ for all f. In this case, noise is attenuated rather than increased in the restoration process. The transfer function for ME can be found by Fourier transformation of the impulse response. This is given by

$$H(\omega) = \left| \frac{\frac{A}{\tau_{ME}} + j\omega A + k_{ME}}{\frac{1}{\tau_{ME}} + j\omega} \right| = \frac{\sqrt{\left(\frac{A}{\tau_{ME}} - k_{ME}\right)^2 + (A\omega)^2}}{\sqrt{\left(\frac{1}{\tau_{ME}}\right)^2 + \omega^2}}. \quad (8)$$

Fortunately, since $k_{ME} < 0$ and $A = 1 - k_{ME}\tau_{ME}$, this function is greater than unity for all frequencies. Thus, inverse filtering is a viable approach for removing ME.

The next issue for removing ME involves implementation of the restoration filter. One approach is to implement the filter in the Fourier domain. However, this method involves Fourier transformation of very large data sets and, as such, is impractical. Implementation in the spatial domain through a convolution operation is necessary. The expression for the restoration filter in the spatial domain is given as

$$w(t) = A\delta(t) - k_{ME} e^{-\left(\frac{1}{\tau_{ME}} + k_{ME}\right)t} \quad (9)$$

where t is again thought of as discretized time or, equivalently, mf.

From the form of this equation, it is apparent that the filter is of infinite extent. For implementation, the filter length must be truncated. A general rule followed here is to truncate the filter at approximately 3000 coefficients. This is roughly three ME time constants and ensures that the error introduced by the truncation is minimal and that ME is still theoretically reduced in amplitude by an order of magnitude. As described above, a convolution operation with a filter length of 3000 elements of differing values

requires a significant computational engine in order to be performed in a reasonable period of time. It is possible, however, to approximate the above exponential filter by a series of steps. The number of steps, their widths, and magnitudes can be varied depending on how closely it is desired to approximate the ideal filter. For example, a six step filter of exponentially increasing step widths with magnitudes equal to the average value of the filter in that interval has been shown empirically to give an excellent correction. Improvements in computational times of two orders of magnitude are possible using this approach while still yielding results that differ insignificantly from those of the ideal filter.

An example of this ME correction method is shown in Figure 3. The figure includes portions of Lake Erie and its accompanying shoreline. It was acquired on April 10, 1984 during a time when ice still bordered the shore. These data have been stretched significantly so that ME is readily observable, and all before and after image pairs in the figure have been stretched identically. Although detector striping is discernible, the bright ice region and homogeneous dark water region form an ideal environment for production of ME. This is clearly observable in Figures 3e and 3g which show Bands 3 and 4 before ME correction. These two bands most strongly exhibit ME in the water region; the alternating light and dark bands, 16 lines wide, are clearly present. Also, the intensity difference between the bands is strongest near the shore, as predicted by the model. Figures 3f and 3h show the same data after ME correction. In Figure 3f, the light and dark bands are virtually absent throughout the entire Band 3 water region. A striping pattern is still present due to the fact that the detector response has not been equalized. The form of the striping pattern is significantly different. The obvious one line wide stripe is due to detector 16 in both bands being slightly "brighter" than the other 15 detectors. Also, coherent noise is noticeable as small vertical dark "bars" within each scan. The correction in Band 4, Figure 3h, suggests that some residual ME may be present. This is due to the fact that Band 4 detectors often saturate in water regions at the low end of their dynamic range. When this happens, assumptions of linearity are no longer valid and the ME response is corrupted by this other phenomenon.

Band 2 also exhibits significant ME as shown in Figure 3c. Although not as pronounced as in Band 3, it is still visually apparent with the largest intensity variation occurring nearest to the shore. Figure 3d shows the same data following ME correction. ME is virtually nonexistent. The slight residual striping pattern is again due to unequal detector response. Lastly, Band 1 also exhibits ME as shown in Figure 3a. In Figure 3b, after ME is removed, the water region is much more clearly defined and subtle changes are more readily apparent.

To complement the qualitative analysis above, quantitative results are shown in Figure 4. The data in Figure 4 were generated by averaging the 400 samples from the water region in Figure 3 in the along scan direction to obtain an average intensity for each detector. These average intensities are plotted as a function of scan index in Figure 4 for one representative detector from each band. The scans are indexed vertically with the top of Figure 3 representing the first scan. Since all data used in the averaging operation were taken from the water region, the assumption is that average variation in the along track direction is very slight and occurs slowly. No significant differences should occur from one scan to the next. However, cursory inspection of the plots show that this is definitely not the case. Before ME correction occurs, a very pronounced sawtooth waveform is evident. This is due to the alternating light and dark intensities produced by ME. Although the magnitude of the fluctuations is small, on the order of 0.5 to 1.0 DN for Bands 2 through 4, it is nonetheless present. After correction, the sawtooth pattern is strongly attenuated. In many cases, a smooth scan to scan variation is evident. In Band 4, for example, the standard deviation for scan to scan difference is 0.5 DN before ME correction. After ME correction, the standard deviation of scan to scan differences is reduced to 0.1 DN. This reduction in variability of 80% indicates, for this example, that 80% of the variability is actually due to instrument artifact and only 20% is due to scene content.

Figure 4 indicates that, for most scans, a correction is made to the "darker" scans to increase their average intensity. This is appropriate for the type of step discontinuity that is present from the brighter ice region to the darker water region (i.e. the detector response has been incorrectly depressed due to ME). If the

step transition were of the opposite direction, as in a transition from a darker to a uniform brighter region, ME would cause the detectors to overshoot. This condition is difficult to observe in typical images since it occurs rather infrequently. It is interesting to note, however, that in Figure 4 the first few scans do not show a sawtooth waveform pattern before correction. Also, the corrected scans are at a significantly higher average intensity than before correction. The reason for this is that in the original image there is a region of ice present on both sides of the water region for the first few scans. As a result, the average intensity is depressed on both the forward and reverse scans. This results in a radiometric error that, while not visible qualitatively, is actually worse since it occurs in all the scans rather than in only half of the scans.

Discussion

Although it can be shown that other artifacts exist, most notably CN and SCS, ME is the most significant artifact contributing to radiometric error in Landsat 5 data. It is also the most noticeable in a visual, qualitative sense. Its removal allows the data user to better utilize the ability of the TM instrument to resolve detail in a radiometric sense.

The magnitude of ME shown in Table 1 comes from the system observing only a calibration pulse. As a result, the magnitude is small. However, from the proceeding analysis, it can be seen that larger pulses will produce correspondingly larger magnitudes of ME in the data. If the worst case situation is considered to be a bright target with an amplitude of 200 DN and duration of 3000 mf (this assumes that the bright target is of a significantly different nature than the normal land regions that Landsat was designed to characterize and also that most users are not interested in data that is more than 50% covered by such features), a maximum radiometric error on the order of 5.2 DN will occur in Band 3 that will take approximately 3000 mf to decay to insignificance (~0.34 DN after three time constants). This represents a

maximum radiometric error on the order of 2%. Maximum errors in Bands 1, 2 and 4 are 2.5, 5.7, and 5.3 DN, respectively.

Because of the long time constant associated with ME, this artifact significantly impacts the information contained in the calibration interval. Calibration pulse values and shutter region bias values will be depressed due to bright scene content. The amount of depression is dependent on the intensity, and duration of intensity, in the scene. For calibration intervals following forward scans, the shutter region is affected more than the calibration pulse. On reverse scans the opposite is true, the calibration pulse is affected to a greater degree than the shutter interval is. As a result, greater variability is introduced into integrated calibration pulse values and an additional error is contained in detector gain estimates. One approach to minimize this is to use only calibration pulses following forward scans. These pulses are located several hundred minor frames from the end of the scene and are, therefore, less affected by ME. However, the best approach is to remove the ME artifact prior to further calibration operations.

It should be pointed out that even after correction of ME, noticeable striping may still be present. This is due to a variety of sources. First, SCS can cause alternating light and dark bands that give the appearance of ME. Second, during the shutter interval a bias correction occurs known as DC restore. DC restore is influenced by the presence of ME and causes a significant change in detector bias. An appropriate method for minimizing both of these effects is to use the shutter region before DC restore occurs to estimate detector bias for the immediately preceding scan.

Lastly, prior to a more complete understanding of ME, other artifacts were supposedly present that are now known to be simply manifestations of ME. The most notable of these was known as scan line droop (Metzler and Malila, 1985, and Kieffer et al., 1985). This artifact was postulated as a "droop" in detector response at the beginning of a scan line, followed by an exponential recovery to a steady state bias level. From the analysis presented here, it is apparent that "droop" was simply the response of the system to a calibration pulse due to ME. Further details are available in Helder et al. (1996).

Conclusions

ME is an artifact most likely caused by circuitry contained in the pre-amplifiers in the analog signal processing chain connecting the detectors to the A/D converters. It can, therefore, be modeled as a first order linear system with an exponential response. The time constant associated with this response is approximately 10 ms which translates to roughly 1040 mf. It is most commonly observed as horizontal bands 16 lines wide of alternating light and dark intensity in homogeneous regions adjacent to sharp across-scan intensity transitions. The magnitude of the ME artifact is such that errors in the data greater than 5 DN can occur. This is a significant radiometric error greater than 2% that decays slowly according to the time constant indicated above. Correction of ME is possible through use of a restoration filter. Fortunately, the transfer function associated with ME has a magnitude greater than unity everywhere and a simple inverse filter can be implemented without introducing additional artifacts or noise. Because of the long time constant associated with ME, the restoration filter requires a length of at least 3000 mf for adequate suppression. To decrease the computational burden required, approximations to the ideal filter are attractive and have been shown to work well.

The approaches presented herein allows users of Landsat 5 data to improve the accuracy of their data sets and are especially attractive to those whose applications are sensitive to small intensity changes. Extensions of these techniques are applicable to Landsat 4 data and will also be used, with some modification, for the analysis of data obtained from Enhanced Thematic Mapper Plus instrument that will fly on Landsat 7.

References

Barker, J.L., "Relative Radiometric Calibration of Landsat TM Reflective Bands," Proceedings of the Landsat-4 Science Characterization Early Results Symposium, Greenbelt, MD, NASA Conference Publication 2355, Vol. 55, No. 3, Feb. 22-24, 1983.

Barker, J.L. and Gunther, F.J., "Landsat-4 Sensor Performance," Proceedings of Pecora VIII Symposium, Satellite Land Remote Sensing Advancements for the Eighties, Sioux Falls, South Dakota, pp. 46-74, October 4-7, 1983.

Crippen, R.E., "A Simple Spatial Filtering Routine for the Cosmetic Removal of Scan-Line Noise from Landsat TM P-Tape Imagery," Photogrammetric Engineering and Remote Sensing, Vol. 55, No. 3, pp. 327-331, March, 1989.

Fusco, L., Frei, U., Trevese, D., Blonda, P.N., Pasquariello, G., Milillo, G., "Landsat TM Image Forward/Reverse Scan Banding: Characterization and Correction," International Journal of Remote Sensing, Vol. 7, No. 4, pp. 557-575, 1986.

Helder, D.L., Quirk, B., Hood, J., "A Technique for the Reduction of Banding in Landsat TM Images," Photogrammetric Engineering and Remote Sensing, Vol. 58, No. 10, pp. 1425-1431, 1992.

Helder, D.L., Barker, J.L., Boncyk, W.C., Markham, B.L., "Short Term Calibration of Landsat TM: Recent Findings and Suggested Techniques," International Geoscience and Remote Sensing Symposium, , Lincoln, Nebraska, May 27-31,1996.

Kieffer, H.H. Cook, D.A., Eliason, E.M., Eliason, P.T., "Intraband Radiometric Performance of the Landsat Thematic Mappers," Photogrammetric Engineering and Remote Sensing, Vol. 51, No. 9, pp. 1331-1350, September 1985.

Metzler, M.D. and Malila W.A. 1985. "Characterization and comparison of Landsat-4 and Landsat-5 Thematic Mapper Data," Photogrammetric Engineering and Remote Sensing, Vol. 51, No. 9, pp. 1315-1330, September 1985.

Murphy, J.M., "Within-Scene Radiometric correction of Landsat Thematic Mapper TM Data in Canadian Production Systems," Proceedings of the Earth Remote Sensing Using Landsat Thematic Mapper and SPOT Sensor Systems, Innsbruck, Austria, SPIE vol. 660, pp. 25-31, April 15-17, 1986.

Poularikas, A.D., and Seely, S., Signals and Systems, PWS Engineering, 1985.

Srinivasan, R., Cannon, M., White, J., "Landsat Data Destriping using Power Spectral Filtering," Optical Engineering, Vol. 27, No. 11, pp. 939-943, November, 1988.

Figure 1. TM calibration interval.

Figure 2. ME due to calibration lamps.

Figure 3. Lake Erie TM scene before and after ME correction.

Figure 4. Scan averages before and after ME correction.

Table 1. ME Parameter Values.

Table 2. Band Average Calibration Pulse Height for Lamp State [111].

Band	Detector	b	k	tau		Band	Detector	b	k	tau
1	1	2.827	0.078	1066		2	1	2.618	0.300	870
1	2	2.519	0.150	1331		2	2	2.039	0.264	1078
1	3	2.474	0.122	1405		2	3	2.209	0.261	1079
1	4	2.468	0.133	676		2	4	2.012	0.308	1076
1	5	2.318	0.124	1516		2	5	2.002	0.258	1143
1	6	2.552	0.137	1095		2	6	2.058	0.243	1124
1	7	2.283	0.124	1104		2	7	2.037	0.296	1064
1	8	2.596	0.127	1322		2	8	2.059	0.303	1190
1	9	2.126	0.103	1304		2	9	2.090	0.298	1142
1	10	2.261	0.109	1482		2	10	2.024	0.276	1206
1	11	2.084	0.111	1198		2	11	2.115	0.213	1360
1	12	2.270	0.103	1475		2	12	2.018	0.301	889
1	13	2.203	0.139	1167		2	13	2.073	0.283	1120
1	14	2.398	0.127	1363		2	14	2.063	0.264	1296
1	15	2.123	0.134	1171		2	15	2.113	0.261	1087
1	16	2.345	0.125	1224		2	16	2.116	0.256	1246
Band average		2.365	0.122	1244		Band average		2.103	0.274	1123
Band std.		0.159	0.013	156.1		Band std.		0.082	0.022	90.25
Band	Detector	b	k	tau		Band	Detector	b	k	tau
3	1	3.335	0.258	1034		4	1	3.280	0.298	927
3	2	2.443	0.192	1282		4	2	2.309	0.202	1074
3	3	2.903	0.192	1143		4	3	2.330	0.230	1005
3	4	2.596	0.372	1036		4	4	2.453	0.247	1116
3	5	2.684	0.318	817		4	5	2.199	0.195	1131
3	6	2.745	0.288	1077		4	6	2.247	0.171	1162
3	7	2.614	0.426	960		4	7	2.174	0.233	906
3	8	2.461	0.116	1125		4	8	2.249	0.250	1159
3	9	2.848	0.297	1127		4	9	2.283	0.257	1049
3	10	2.559	0.232	972		4	10	2.239	0.208	1348
3	11	2.726	0.346	1044		4	11	2.384	0.242	1052
3	12	2.615	0.190	1173		4	12	2.241	0.258	1261
3	13	2.542	0.346	1079		4	13	2.366	0.231	1114
3	14	2.557	0.199	1467		4	14	2.326	0.240	1154
3	15	2.580	0.263	1081		4	15	2.244	0.222	1247
3	16	2.577	0.211	1212		4	16	2.470	0.290	1147
Band average		2.674	0.265	1102		Band average		2.362	0.236	1116
Band std.		0.150	0.067	102.0		Band std.		0.143	0.024	85.41

Table 1. ME Parameter Values

Band	Average Pulse Height	Standard Deviation
1	216.5	5.72
2	196.4	10.95
3	207.0	2.20
4	182.1	8.4

Table 2. Band Average Calibration Pulse Height for Lamp State [111].